Contract No:

This document was prepared in conjunction with work accomplished under Contract No. 89303321CEM000080 with the U.S. Department of Energy (DOE) Office of Environmental Management (EM).

Disclaimer:

This work was prepared under an agreement with and funded by the U.S. Government. Neither the U.S. Government or its employees, nor any of its contractors, subcontractors or their employees, makes any express or implied:

1) warranty or assumes any legal liability for the accuracy, completeness, or for the use or results of such use of any information, product, or process disclosed; or
2) representation that such use or results of such use would not infringe privately owned rights; or
3) endorsement or recommendation of any specifically identified commercial product, process, or service.

Any views and opinions of authors expressed in this work do not necessarily state or reflect those of the United States Government, or its contractors, or subcontractors.

Safeguards Technology Development Program
FY2021 Annual Report
September 30th, 2021

Report Title: Production of Particle Reference and Quality Control Materials FY21 Annual Report

WBS # – Project Title:
24.1.3.4 – Development of New Particle Working Standards for NWAL Particle Laboratory Calibration and Quality Control

HQ Team Lead and PM:
HQ Team Lead - Arden Dougan, HQ PM - Ning Xu

Project PIs, Contributing Staff, and Affiliations:

Spencer M. Scott[1], Aaron T. Baldwin[1], Michael G. Bronikowski[1], Michael A. DeVore II[1], Laken A. Inabinet[1], Wendy W. Kuhne[1], Benjamin E. Naes[2], Ross J. Smith[1], Eliel, Villa-Aleman[1], Kimberly N. Wurth[2], Bruce W. Arey[3], Heather S. Cunningham[3], Eirik J. Krogstad[3], Kelly McHugh[3], Matthew J. Olszta[3], Timothy R. Pope[3], Riane E. Stene[3], May-Lin L. Thomas[3], Stephan K. Vogt[3], Mindy M. Zimmer[3], Chelsie L. Beck[3], Wilaiwan M. Chouyyok[3], Travis J. Tenner[2] (PI), Christopher A. Barrett[3] (PI), and Matthew S. Wellons[1] (PI)

[1] Savannah River National Laboratory, Aiken SC

[2] Los Alamos National Laboratory, Los Alamos NM

[3] Pacific Northwest National Laboratory, Richland WA

Executive Summary:

A DOE laboratory team composed of SRNL, PNNL, and LANL have continued method development for, and the production of, fit-for-purpose QC particulates as requested by the IAEA. NIST has provided technical guidance as a collaborative SME role to the effort. In FY21, the team performed R&D focused on a combination of 1) reference material particle production, 2) formulation of feedstocks with tailored elemental and isotopic composition, 3) advanced analytical methods to characterize development specimens and qualify products, and 4) production and delivery of completed QC particulate or calibration material batches. In detail:

- PNNL delivered 1A/1B QC particulate materials qualification report, PNNL- 30762, and a follow-up addendum on PNNL particle sample preparation, PNNL-30984.
- PNNL completed method development of UTEVA separation with U/Th and successfully demonstrated this protocol with the repurification of CRM U630 and subsequent synthesis of representative particles using this material.
- PNNL's investigation of uranyl acetate recrystallization identified the removal of ingrown Th in samples of uranyl nitrate. This drove the establishment of a new synthesis protocol for blended CRM material using a nitrate chemical form.
- SRNL delivered 1A/1B QC particulate materials to the IAEA's ESL, including an accompanying qualification report, SRNL-STI-2021-0070, supported by LG-SIMS analysis by LANL.

- SRNL completed method development of mixed actinide particulates using U/Th surrogates in support of U/Pu production development efforts, with accompanying SIMS analysis by LANL; these efforts are captured in the report SRNL-TR-2021-00663.
- SRNL installed the THESEUS particle generation platform within a CAT II nuclear facility and conducted an initial demonstration of mixed U/Pu particle generation, resulting in the shipment of particulate samples to LANL for SIMS analysis.
- Two publications were submitted for publication as part of the INMM & ESARDA joint meeting in August 2021 and were entitled "Scale-up And Production Of Uranium-bearing QC Reference Particulates By An Aerosol Synthesis Method" with document #SRNL-STI-2021-00350, and "Aspects Of Crystal Growth And Atomic-Scale Characterization Of U/Th Age-Dating Particles", with document #PNNL-SA-164937.

FY21 Project Summary:

U/Th Chronometry Particle Generation and Characterization Activities

The project focus for PNNL in FY21 centered around method development in the areas of particle synthesis, actinide separation chemistry, and formulation of suitable age-dating reference material. With a goal of developing reference particles for $^{234}U/^{230}Th$ radiochronometry, the chemical methods developed for the 1A/1B and 2A/2B production cycles would need to be evaluated and potentially altered to meet the requirements of a future 4A/4B production cycle. The previously established PNNL technique of hydrothermal synthesis of UO_2 particles was optimized for uranyl acetate precursor. Tailoring this method for larger particle sizes was achieved with adjustments to reaction time and precursor concentration. The co-crystallization of U and Th in a dioxide form was found to readily occur in a hydrothermal synthesis. A study of several batches of UO_2 particles spiked with increasing concentrations of natural Th showed a linear doping trend when measured by bulk ICPMS analysis. Elemental homogeneity in individual UO_2 particles spiked with natural thorium was also evaluated with STEM and SEM/EDS, and found to be uniform in all cases. The overall findings of this initial study affirmed the use of the standard hydrothermal synthesis of UO_2, with Th nitrate spiking, as an efficient route to $Th_{1-x}U_xO_2$ reference particles (Figure 1). The results of this study were presented at the INMM & ESARDA joint meeting and published as a conference proceeding under information release number PNNL-SA-164937. Using this chemical strategy, repurified stocks of uranium converted to uranyl acetate could be spiked with SRM 4342a (^{230}Th standard) to generate age-dating UO_2 particles with synthetic ages.
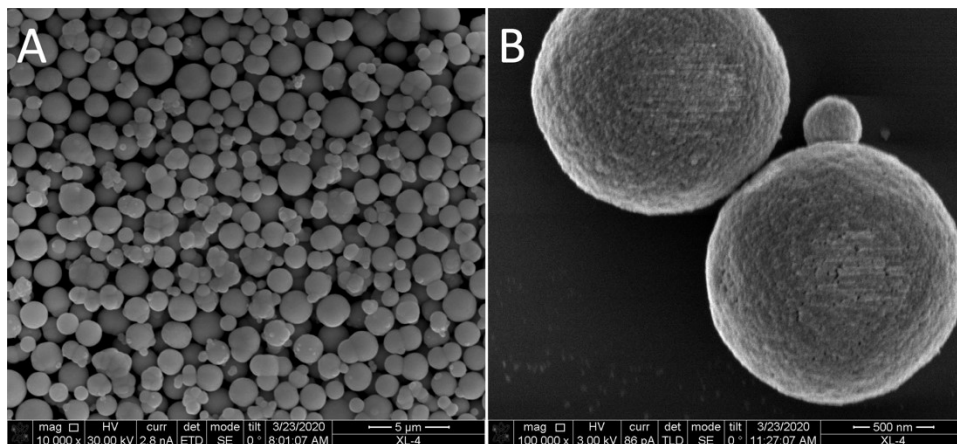

Figure 1. SEM images collected on samples of Th-doped UO_2 particles prepared with standard hydrothermal synthesis.

While certainly a viable approach for the direct introduction of Th into UO_2 particles, the use of uranyl acetate as the primary precursor for hydrothermal synthesis using blends of CRM was discovered to be unfeasible. Initial indications of Th decontamination in uranyl acetate precursor were observed in samples of UO_2 particles synthesized from blended CRM sent to NIST for LG-SIMS evaluation and age-dating determination. The particles were diluted to a 20 ppm concentration and applied to one silicon wafer and one vitreous carbon planchet. The team used PNNL's drop-casting technique to maximize the separation of individual particles and minimize particle agglomeration and coffee-ring clusters. The planchets were evaluated by helium ion microscopy (HeIM) prior to shipment and found to contain a sufficient concentration of well-separated UO_2 particles (Figure 2). Details for this method were reported to the IAEA as part of an addendum (PNNL-30984) to the more extensive characterization report for 1A/1B UO_2 particles (PNNL-30984).
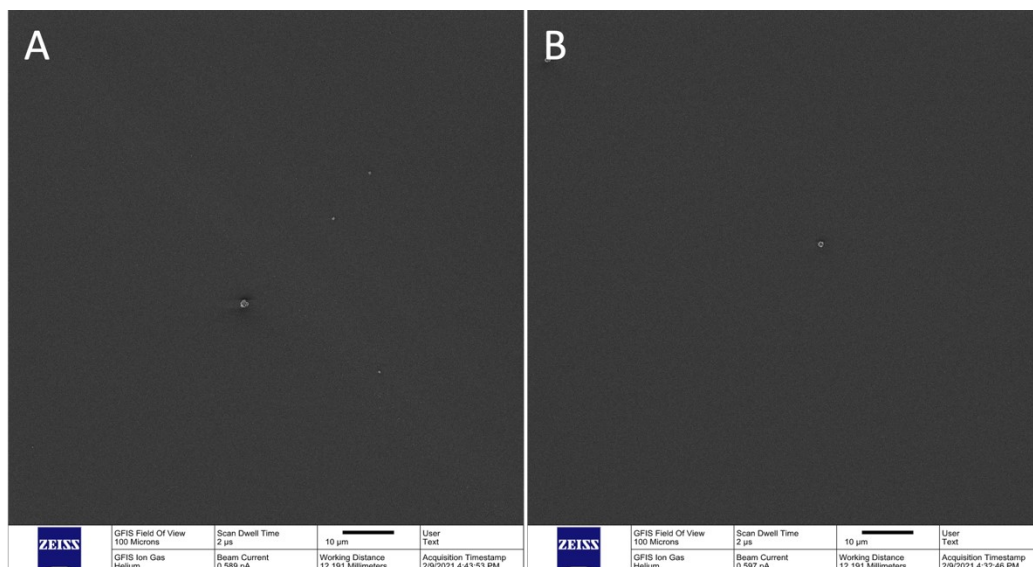

Figure 2. Images collected from representative UO_2 particles on silicon prepared for NIST.

The NIST evaluation reported that the particle-to-particle isotopics for this sample set appeared homogeneous and consistent with bulk values measured by TIMS at PNNL. When summing isotopic values (Table 1) and performing a chi-squared test against bulk isotopic measurements, most particles were found to have chi^2 values of less than or equal to 1. However, it was noted that ^{234}U isotopic values were more scattered than even the lower abundance ^{236}U isotope for 3 of the 14 particles measured, which may have been due to slight variations in particle size. $^{234}U/^{230}Th$ ratio measurements proved too challenging to perform as there wasn't a high enough concentration of Th in the particles for accurate ^{230}Th measurements. While larger particle sizes may have helped with this limitation, the lower-than-expected thorium concentration would be an issue for any future production cycles. The same batch of particles was later analyzed by MC-ICP-MS at PNNL, with no detectable amounts of thorium measured, confirming earlier observations.

Table 1. Uranium/Thorium assay and isotopic analysis from LG-SIMS microbeam of individual UO2 particles.

ID#	^{230}Th Age* yrs	1s	95% conf. (yrs) lower	upper	^{230}Th Cts	^{234}U Cts	^{234}U %	1s %	^{235}U %	1s %	^{236}U %	1s %	^{238}U %	1s %	Count Time (s)	Corr. Counts	Analysis Date	Birth Date
1	-12.7	27.8	0.0	92.4	0	2370	0.00961	0.00048	1.0335	0.0096	0.00206	0.00026	98.9549	0.0097	400	-0.57	4/8/21	12/5/33
2	3.9	11.5	0.0	58.1	1	5732	0.00881	0.00050	1.0305	0.0068	0.00208	0.00020	98.9587	0.0071	400	0.43	4/8/21	5/5/17
3	37.3	65.8	0.0	373.0	1	925	0.00869	0.00066	1.0479	0.0115	0.00211	0.00046	98.9413	0.0115	240	0.66	4/9/21	12/23/83
4	184.9	438.8	0.0	2311.5	1	146	0.01204	0.00367	1.0605	0.0472	0.00168	0.00132	98.9258	0.0470	340	0.51	4/9/21	4/29/183
5	-35.4	98.8	0.0	356.6	0	635	0.00688	0.00117	1.0243	0.0253	0.00287	0.00065	98.9660	0.0250	300	-0.43	4/9/21	9/18/56
6	35.5	62.6	0.0	354.9	1	972	0.00938	0.00101	1.0575	0.0100	0.00211	0.00048	98.9310	0.0099	240	0.66	4/9/21	10/12/85
7	-19.6	57.9	0.0	212.4	0	1073	0.00967	0.00103	1.0285	0.0107	0.00238	0.00058	98.9595	0.0110	280	-0.40	4/8/21	11/4/40
8	-34.6	137.2	0.0	539.1	0	434	0.00848	0.00115	1.0307	0.0120	0.00257	0.00067	98.9582	0.0121	200	-0.29	4/8/21	11/4/55
9	-28.9	97.8	0.0	371.3	0	622	0.01094	0.00138	1.0503	0.0100	0.00120	0.00032	98.9375	0.0100	240	-0.34	4/8/21	3/20/50
10	3.9	8.7	0.0	46.8	1	7246	0.00954	0.00029	1.0325	0.0044	0.00209	0.00011	98.9559	0.0043	320	0.54	4/8/21	5/2/17
11	-113.5	494.9	0.0	1978.5	0	119	0.00995	0.00225	1.0255	0.0229	0.00236	0.00080	98.9622	0.0232	180	-0.26	4/8/21	10/10/34
12	-66.9	291.5	0.0	1165.5	0	202	0.00757	0.00209	1.0318	0.0273	0.00181	0.00081	98.9589	0.0271	180	-0.26	4/8/21	2/16/88
13	-375.4	1821.0	0.0	7404.7	0	32	0.00350	0.00243	1.1668	0.0654	0.00211	0.00182	98.8276	0.0649	160	-0.23	4/8/21	8/28/96
14	-38.2	113.0	0.0	414.5	0	550	0.00682	0.00133	1.0514	0.0179	0.00166	0.00056	98.9401	0.0180	280	-0.40	4/8/21	6/19/59
All	-0.9	8.0	0.0	14.7	5.0	210581	0.00921	0.00023	1.0364	0.0029	0.002043	0.000082	98.9521	0.0029	3760	-0.37	4/8/21	3/13/22

The reduced levels of thorium were traced back to the process of generating uranyl acetate from blended CRM, which is performed in nitric acid media. Once an appropriate uranium isotopic blend is achieved, several sequential steps are used for chemical conversion, starting with the evaporation of uranyl nitrate solution, multiple calcination and oxidation treatments at high temperatures (Figure 3A), dissolution of the resulting UO_3 powder in glacial acetic acid (Figure 3B), and finally crystallization of uranyl acetate dihydrate.
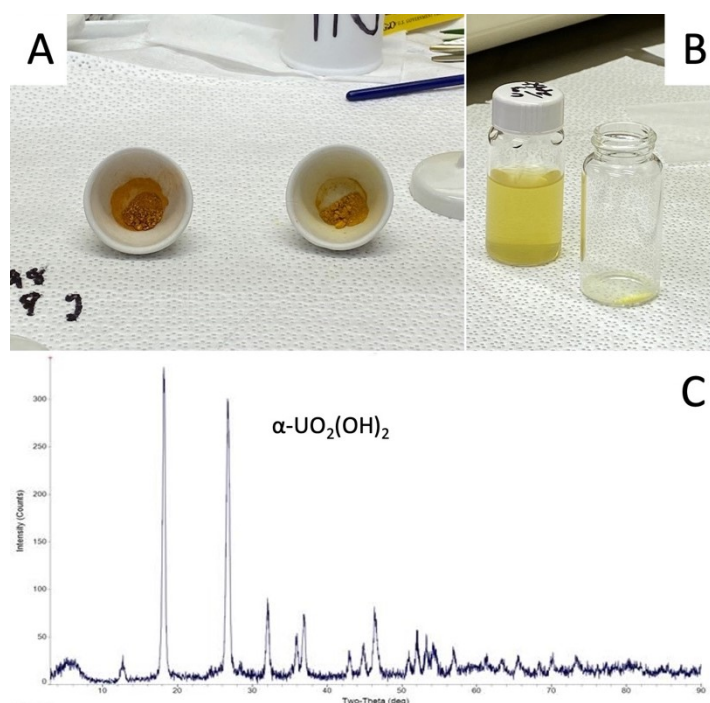

Figure 3. A) Calcination uranium oxide powder, B) vials of uranium acetate solution and dried crystals, and C) powder XRD pattern of a sample of α-UO₃ that hydrolyzed in air over a period of 2 months.

Dissolution of uranium oxide in acetic acid is facilitated by first forming the hexavalent uranium trioxide (UO_3) using calcination. XRD analysis was used to monitor the conversion of uranium from nitrate to

trioxide in between calcination treatments. Three routes to the preparation of UO_3 were explored based on the findings of a previous PNNL report (PNNL-20951). From our studies of $UO_2(NO_3)_2$ conversion to α-UO_3, we found that this chemical transformation can take place at temperatures ranging from 350-470℃ over a period of several days. To ensure homogeneity in each sample, powders were allowed to cool and then ground in a mortar and pestle for several minutes before repeating the calcination step once again. XRD analysis found that if α-UO_3 powders are stored in normal atmosphere, a hydrolysis product of α-$UO_2(OH)_2$ will form within a few weeks (Figure 3C). The resulting α-UO_3 powder is readily dissolved in acetic acid but must undergo a crystallization and filtration step to isolate uranyl acetate dihydrate from the mother solution. It was found that much of the thorium fraction is lost during filtration, impacting the relative age of the uranium product. Because of this process, naturally ingrown [230]Th was found to be much lower than calculated values due to the acetate recrystallization.

To preserve ingrown [230]Th in various blends of CRM, a new method of synthesizing uranium oxide particles directly from uranyl nitrate powder was investigated. In past PNNL production cycles of uranium particle reference materials for the IAEA Environmental Sample Laboratory, the chemical purity of the uranium precursor was found to change the resulting particle crystallinity and morphology dramatically. Instead of forming spherical polycrystalline UO_2 particles, octahedral-shaped, single-crystal UO_2 particles were grown with identical reaction conditions. The removal of impurities, such as uranium carbonate, resulted in the growth of octahedral-shaped particles, as shown in (Figure 4). In qualification and proficiency testing with LG-SIMS, the uniformly dense single-crystal UO_2 particles showed much longer-lived signal intensities when compared to polycrystalline UO_2 particles. To this end, a more purposeful strategy for the synthesis of single-crystal particles was explored for [234]U/[230]Th age-dating reference material with uranyl nitrate as a starting precursor, and a technique referred to as microwave-assisted hydrothermal synthesis.
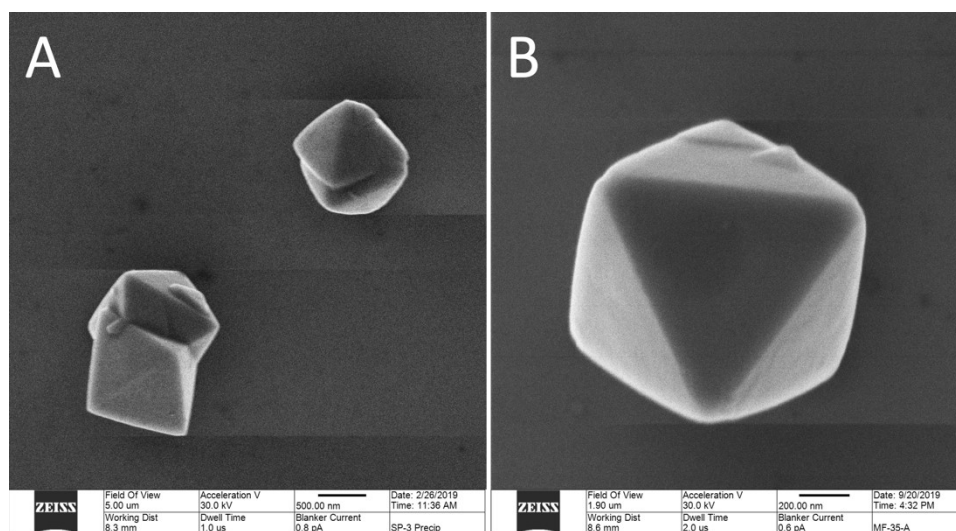

Figure 4. Helium ion images of octahedral-shaped, single-crystal UO_2 particles.

Traditional hydrothermal synthesis is typically performed in a Teflon-lined, stainless-steel autoclave. The vessel is heated through convection in an oven or furnace to reach appropriate growth temperatures, slowly ramping to the desired setpoint for crystal growth. As the term implies, microwave-assisted hydrothermal synthesis uses specific microwave frequencies to heat the reaction solution directly and rapidly in an autoclave. The resulting temperature ramp profile is much steeper, with greater control of

setpoints afforded with internal infrared sensors. To test these augmented capabilities, a series of cerium oxide syntheses were conducted. As many other reports have documented, ceria is the preferred non-radioactive analog for uranium oxide, which crystallizes with the same fluorite crystal structure. In a typical procedure, $Ce(NO_3)_3 \cdot 6H_2O$ (0.0753 g) and PVP (0.0378 g) were dissolved in a mixed solvent of anhydrous ethanol (1.5 mL) and deionized water (15.3 mL) in 100 mL Teflon vessels. The mixed solution was ultrasonically agitated for 5 min at room temperature and then transferred into a high-pressure vessel, sealed, and was subjected to microwave treatment at 180°C for 30 min, with a power of 6 W using an Anton Parr Microwave Go. After cooling, the precipitated material obtained from the reaction vessel was collected and washed several times with deionized water and absolute ethanol. Residual PVP surfactant was removed with successive washing steps with Vertrel.
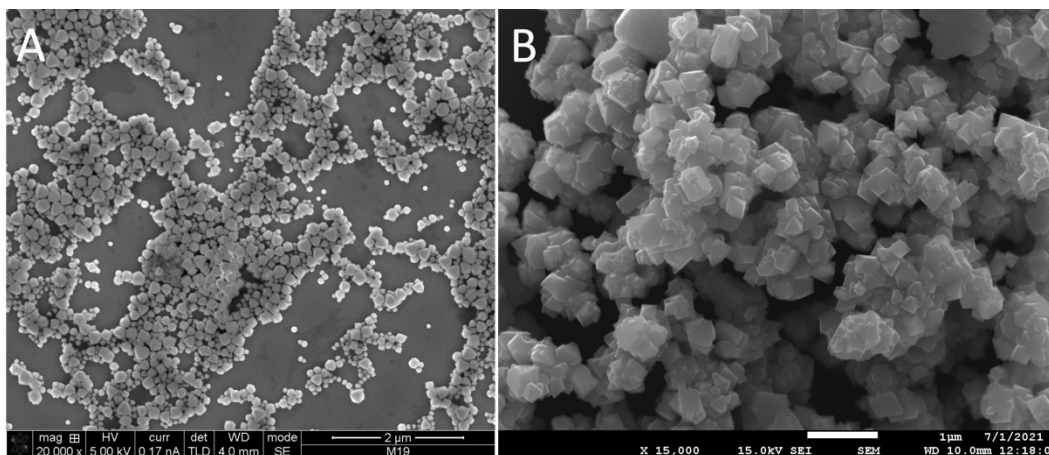

Figure 5. SEM images of CeO2 (A) with PVP (4:1 molar ratio of PVP:Ce) and (B) without PVP.

The majority of the resulting CeO_2 particles were found to have a distinct octahedral-shaped morphology, as can be seen in Figure 5A. As previously seen with single-crystal UO_2 particles, the isotropic crystal growth of compounds with a fluorite lattice structure generally develops into an octahedron, enclosed by eight (111) facets. An SEM survey of particle size found a range of 50-200, with larger particles having a much more apparent octahedral shape. Unlike the previous hydrothermal method, this synthesis protocol utilizes a surfactant as a structure-directing ligand. Removal of the surfactant from the reaction results in the formation of larger, micron-sized particles, shown in Figure 5B. However, crystalline agglomerates, several microns in size, form a significant fraction of the sample without a surfactant.
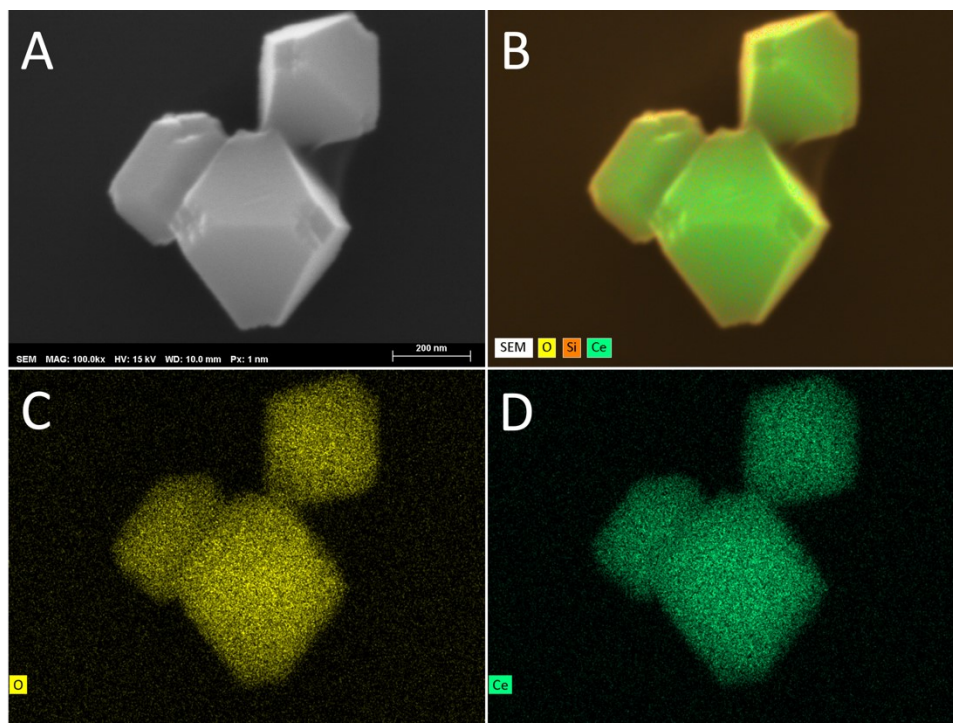
Figure 6. SEM and corresponding EDS mapping of CeO$_2$ particles after 6 hrs of microwave treatment at 180 °C. (A) the original SEM image of CeO$_2$, (B) combined elemental analysis result from Si and O and Ce, (C) elemental map of oxygen, and (D) Ce.

Higher magnification SEM imaging identified residual PVP surfactant adhered to CeO$_2$ particles despite numerous washing treatments (Figure 6A). Calcination of particle material in air at 400 °C was found to remove any remaining organic material. EDS mapping, highlighted in Figure 6C and Figure 6D, confirmed the singular chemical composition of cerium oxide, with no other detectable impurities.
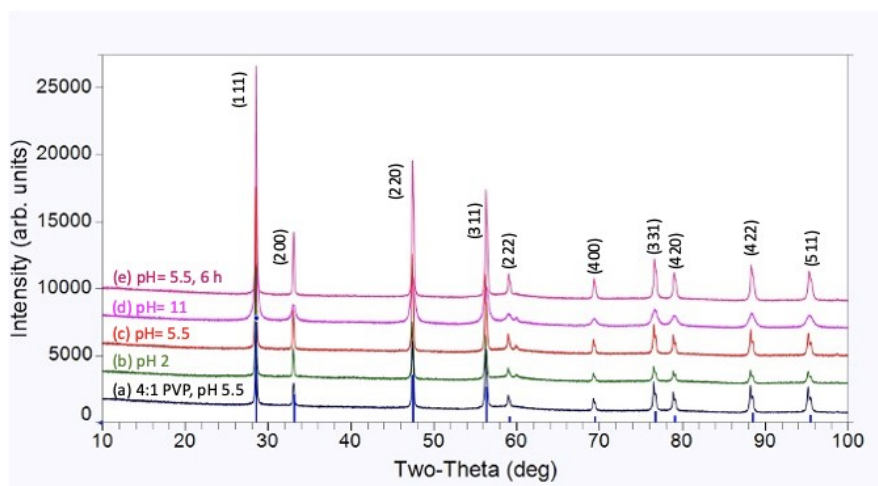

Figure 7. XRD of (A) 4:1 ratio of PVP, (B) no surfactant but pH adjusted to 2, (C) no surfactant, no pH adjustments, (D) no surfactant but pH adjusted to 11, and (E) longer reaction time of 6 hrs. Reference (blue line) cerianite Ce•CeO$_2$.

The crystallinity of as-synthesized CeO$_2$ particles (pH 5.5) and several other batches of particles synthesized without PVP surfactant and/or adjusted solution pH was determined by XRD analysis. The

strong and sharp diffraction peaks in Figure 7 indicate highly crystalline material in all samples. The XRD pattern can be indexed to pure face-centered cubic (FCC) fluorite CeO_2 with a lattice constant of a = 5.41 Å (JCPDS card no. 34-0394). XRD observed no additional peaks or changes in peak width for pH-adjusted conditions.
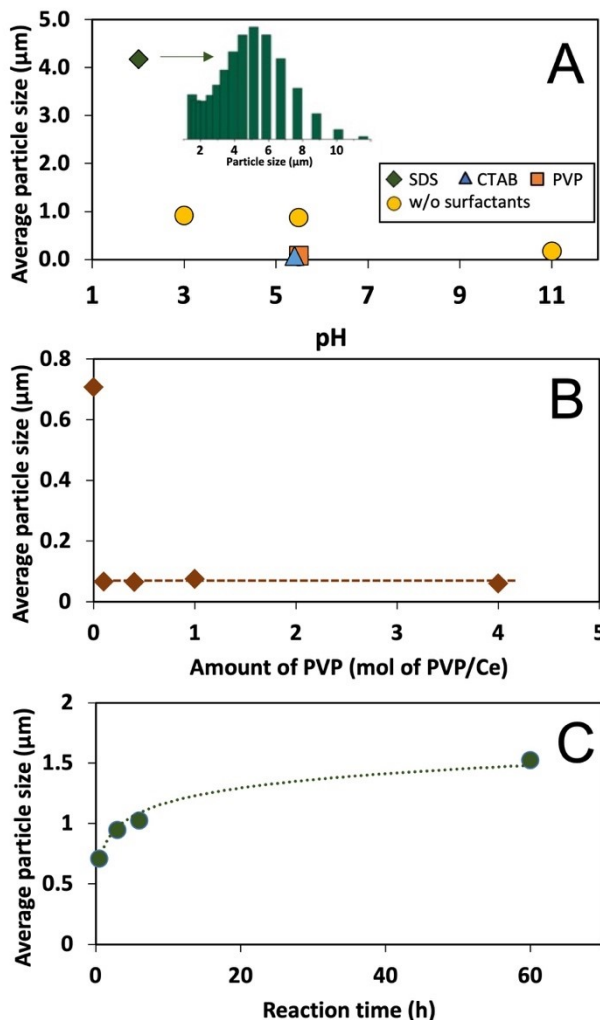

Figure 8. Average CeO_2 particle sizes vs. (a) pH after 30 min of microwave treatment (180 °C), (b) amount of PVP, (c) reaction time. Average particle sizes measured by laser diffractometry, inset graph in (a) shows particle size distribution.

With the addition of PVP surfactant dictating the resulting particle size of as-synthesized CeO_2 particles, a series of alterations were made to the reaction conditions in an effort to control particle size. Four main factors were investigated: solution pH, surfactant concentration, reaction time, and surfactant type. In the case of the latter variable, the addition of SDS and CTAB disrupted the formation of octahedral-shaped particles, resulting in large agglomerates in the case of SDS, and nanoparticles when using CTAB. Bulk particle size analysis (Figure 8A) collected by laser diffractometry measured an average particle size for SDS and CTAB ceria particles at approximately 5 μm and 20 nm, respectively. Impact due to reaction pH was also studied, with an increase of average particle size of about 1 μm noted at pH 3 and 5.5, and no measurable size change at pH 11. To remove contributions due to surfactant, PVP was omitted in all cases. Changes to the molar ratio of PVP/Ce, outlined in (Figure 8B), resulted in little to no change in particle size

with increasing PVP concentrations. However, as previously noted, the complete removal of PVP increased the average diameter to ~700 nm. Figure 8C shows the change in ceria particle size as a function of reaction time. As can be seen, particle size is quickly defined in the first few hours of the reaction, with extending heating times out to 60 hours only increasing the average particle size to 1.5 μm.
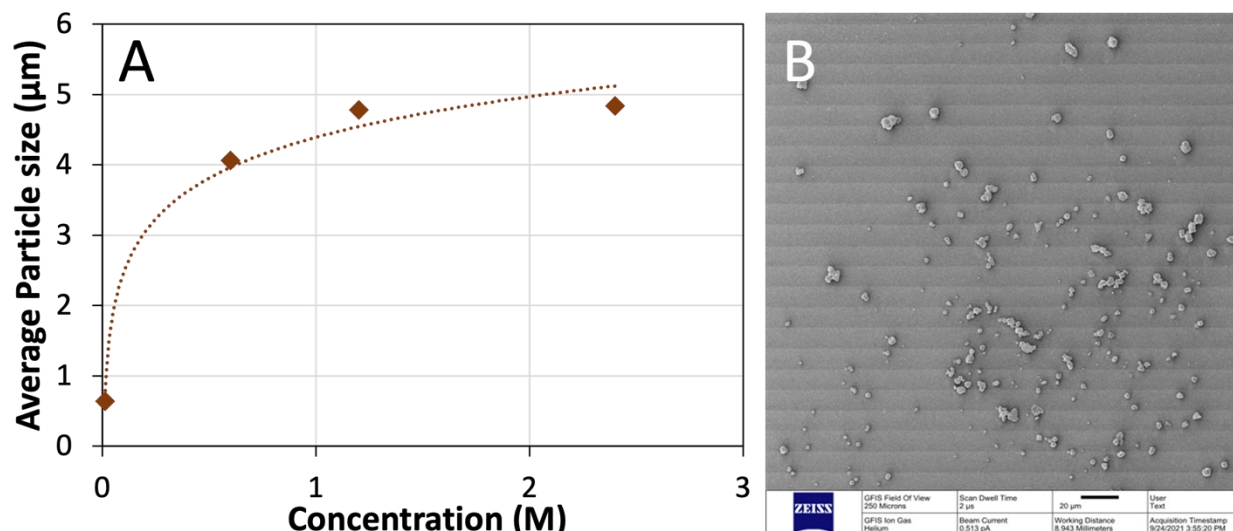

Figure 9. A) Average particle size (measured by laser diffractometry) as a function of short-chain PVP (3500) concentration. B) HeIM image of representative CeO₂ particles grown with PVP3500.

Given the necessity for some amount of capping ligand to mitigate particle clustering and secondary nucleation, the impact of shortened PVP chain lengths was investigated with respect to average particle size. Contributions from the chain length of PVP were examined using three different molecular weights of PVPs (3500, 8000, and 55000). When a short-chain PVP (3500) was used in combination with a standard 3 hour, microwave-assisted hydrothermal synthesis, the resulting average particle size was measured at approximately 637 nm (+/- 22 nm). For the two longer chain lengths, average particles sizes of 66 and 113 nm for reactions performed with 55000 and 8000 PVP chain lengths, respectively. The significant increase in particle size for PVP3500 matched dimensions measured for particles with no PVP added; however, aggregation and clustering seen in the case of the latter were not observed when using short-chain PVP. The direct correlation between capping ligand chain length and particle size was further extended with a short-chain PVP concentration study (Figure 9A). Vastly increasing the concentration of PVP3500 ligand gives a corresponding increase in particle size, plateauing at around 5 μm. The pounced size-effect was found to occur because of changes to the crystal growth mechanism, where polycrystalline particles were formed instead of single-crystal octahedra (Figure 9B).

Having thoroughly explored the different reaction parameters to the new microwave-assisted hydrothermal synthesis process with cerium nitrate, the focus was shifted back to uranium particle synthesis. Uranium nitrate precursor was used in place of cerium for a typical 30-minute reaction at 180°C using PVP3500 as a capping ligand. It was noted that upon extraction and washing of the final product, a purple to brown pearlescence could be observed when agitating the colloidal suspension. UO_2 particles typically present as a black powder/suspension, so this observation suggested the presence of uranyl hydrate species, such as schoepite. On closer examination of this product using HeIM imaging, a unique, disc-like morphology was found for individual particles. Most of the particles had an oval shape 1-2 μm in

length and 0.5-1 μm in width, with particle thickness ranging from 200-500 nm. Further analysis is currently underway to identify the primary chemical composition and relative crystallinity of these particles. Based on previous work, pH adjustments will need to be made to tailor the synthesis towards oxide formation, as disc/platelet morphologies are typically observed for hydrated forms of uranium, owing to a reaction pH of 8 or higher.
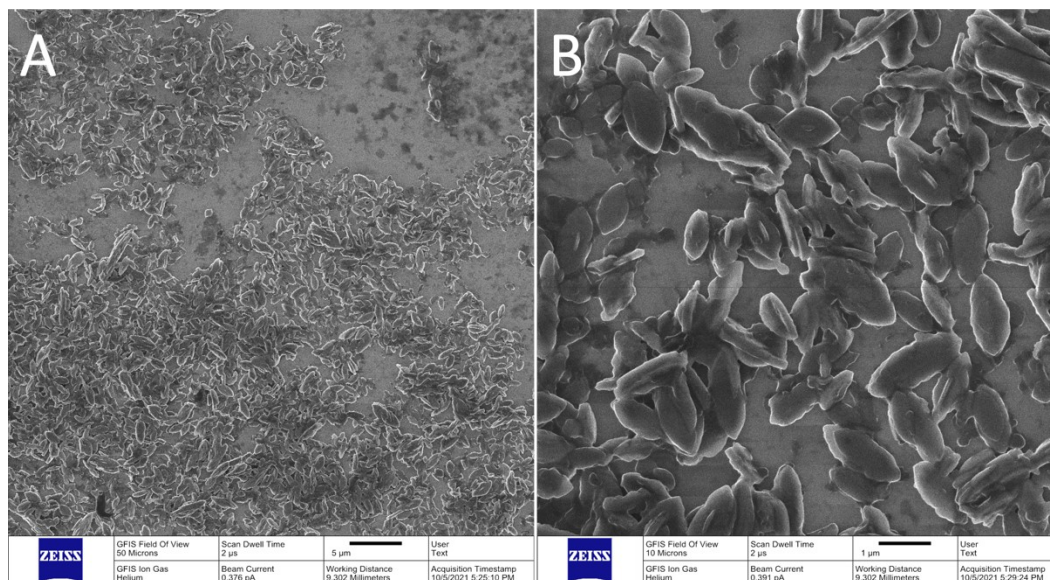

Figure 10. HeIM images collected from a sample of uranium oxide particles synthesized with uranyl nitrate and PVP.

In parallel to the material science and characterization tasks executed under this project, repurification of uranium precursor material was performed with the goal of generating a stock of recently decontaminated feedstock. Per the need to develop suitable reference materials for uranium particle age determination, including new materials that could be repurified at regular intervals [1], PNNL successfully performed chemical separations of uranium from thorium on a pristine aliquant of uranium CRM-630. CRM-630, a highly enriched uranium with an isotopic content of 63% ^{235}U, has a verified time of production, i.e., the last time a chemical purification occurred, on June 6, 1989[2]. The aliquant of CRM-630 received was gravimetrically split into two fractions:

- One aliquant of about 5 mg of the original uranium CRM-630 was left unseparated to produce a particle batch with a nominal age of about 32 years[2]
- The second aliquant of about 9.30 mg of uranium was chemically separated using Eichrom UTEVA extraction resin. The uranium and thorium masses loaded onto the column are indicated in Table 2 with the subscript "load" and after-separation recoveries with the subscript "recovery". Recoveries for both uranium and thorium are close to 100%, indicating the high separation efficacy of Eichrom UTEVA. A separation coefficient could not be quantified because of the ultra-trace amounts of thorium in the uranium fraction, if any
- A thorium recovery of 97% suggests that no more than 0.16 ng of ^{230}Th was left unseparated in the uranium fraction. However, it is more likely that this fraction is eluted from the extraction column

---

[1] 2019 IAEA Technical Meeting on Particle Analysis of Environmental Samples for Safeguards Purposes: Recommendations, No 17.

[2] Certified Reference Material CRM U630 (1g) Uranium (U_3O_8) Isotopic Standard, 63% U-235, 1 gram U, NBL PO (2020).

in the pre-wash. An unseparated quantity of 0.1 ng of ^{230}Th in the uranium fraction would result in an apparent age of the material of about one year

Table 2. Uranium and thorium loads and recoveries from CRM-630.

U$_{load}$ [mg]	U$_{recovery}$ [mg]	^{230}Th$_{load}$ [ng]	^{230}Th$_{recovery}$ [ng]
9.30±0.10	9.59±0.29	5.11±0.07[†]	4.95±0.58[‡]

[†]Th load calculated based upon Th-230 in-growth from U-234 decay assuming a nominal "age" of 32 years. [‡]Recovery based upon the total Th and Th-232/Th-230 ratio of 0.3 as measured on two separate aliquants of the recovered Th fraction and two different instruments.

The PNNL separation team affirmed that the chemical separation protocol developed for age-dating effectively removed ingrown ^{230}Th, formed since its original production, i.e., resetting its ^{234}U/^{230}Th "clock" to a nominal age of zero. In future work, this thorium-free, highly enriched uranium will be used as a base material to produce particles with "synthetic" ages between 0 and 40 years. In order to accomplish this task, two units of NIST SRM 4342a[3], a reference material with a nominal massic activity of 40.8 Bq/g of ^{230}Th and a total of 5.16 g of solution per unit, were acquired and analyzed inhouse. Proposed particle production of uranium materials for U/Th age dating are as follows:

1. **NBL CRM-630**

   The unseparated aliquant of CRM-630 will deliver HEU particles with a nominal age of about 32 years[2].

   Mixing of the thorium-free CRM-630 aliquant with SRM 4342a can deliver uranium particles with "synthetic ages" between T = 0 years and T = 50 years. Table 3 presents the isotopic composition and ages of three suggested production batches. These are indicated as CRM-630-0 (freshly separated U with a separation date of September 1, 2021), CRM-630-10 (with an added ^{230}Th amount to simulate an age of about ten years), and CRM-630-20 (with an added ^{230}Th amount to simulate an age of about 20 years or older).

2. **IRMM1000a**

   This material was selected for the production of U/Th age dating particles because of its certified age of about nine years (chemical separation date 2012-07-09)[4]. This CRM was produced by JRC G.2 (formerly IRMM) from low-enriched uranium with a relative mass fraction m(^{235}U)/m(U) of 3.6 % and a uranium mass of about 20 mg per unit.

   PNNL acquired two units of IRMM1000a and planned to produce one uranium particle batch from the original material with a nominal ^{234}U/^{230}Th based age of 9 years. As the exact uranium isotopic composition of IRMM1000a is not stated on the certificate, PNNL will characterize the major and minor uranium isotopic abundances using its in-house HR-MC-ICP-MS measurement capability. The final product that can be made available to the IAEA are particles of low-enriched uranium with a well-characterized uranium isotopic composition and a ^{234}U/^{230}Th based age of about nine years (see Table 3).

3. **2A/2B**

---

[3] Certificate, Standard Reference Material® 4342A Thorium-230 Radioactivity Standard, NIST (2007).
[4] Certificate, Certified Reference Material IRMM-1000a, JRC G.2 (2017).

Other workable CRM recipes can utilize the **2A/2B** feedstock solutions that will be prepared at SRNL later in 2021. The request for the 2A/2B production by the IAEA calls for one LEU feedstock solution having a $n(^{235}U)/n(U)$ slightly below 20% and a second HEU feedstock solution with a $n(^{235}U)/n(U)$ slightly above 20% (see Table 3).

A similar approach used for CRM-630 will allow for the production of 2A/2B particle batches with varying synthetic production ages. The unseparated 2A/2B batches will have an approximate nominal age of T = 58 years, based on the production dates of the three CRMs used for the 2A/2B feedstock preparation. A portion of the feedstock solution will be chemically separated and mixed with exactly known quantities of SRM 4342a. These mixes are indicated in Table 3 as 2A/2B-0 (freshly separated uranium with a stated separation date), 2A/2B-10, a synthetic blend of the newly separated 2A/2B uranium fraction with SRM 4342a to simulate an age of T = 10 years, and 2A/2B-20, a synthetic mix of the freshly separated 2A/2B uranium fraction with SRM 4342a to simulate an age of T = 20 years.

Table 3. Proposed uranium particle materials for $^{234}U/^{230}Th$ age dating.

Material	^{234}U [at-%]	^{235}U [at-%]	^{236}U [at-%]	^{238}U [at-%]	Purification date	"age" [y]	$^{234}U/^{230}Th$ [at/at]
CRM-630[1]	0.6135	63.0690	0.9621	35.3560	06/06/1989	32 y	$9.03 \cdot 10^{-5}$
CRM-630-0[1]	0.6135	63.0690	0.9621	35.3560	09/01/2021	(0 y)	0
CRM-630-10[1]	0.6135	63.0690	0.9621	35.3560	09/01/2021	(10 y)	$2.82 \cdot 10^{-5}$
CRM-630-20[1]	0.6135	63.0690	0.9621	35.3560	09/01/2021	(20 y)	$5.65 \cdot 10^{-5}$
IRMM1000[2]	n/a	3.6	n/a	n/a	07/09/2012	9 y	$2.54 \cdot 10^{-5}$
2A[3]	0.17	19.5	0.02	80.3	n/a	58 y	$1.6 \cdot 10^{-4}$
2B[3]	0.17	20.1	0.02	79.7	n/a	58 y	$1.6 \cdot 10^{-4}$
2A-0[3]	0.17	19.5	0.02	80.3	TBD	(0 y)	0
2B-0[3]	0.17	20.1	0.02	79.7	TBD	(0 y)	0
2A-10[3]	0.17	19.5	0.02	80.3	TBD	(10 y)	$2.82 \cdot 10^{-5}$
2B-10[3]	0.17	20.1	0.02	79.7	TBD	(10 y)	$5.65 \cdot 10^{-5}$
2A-20[3]	0.17	19.5	0.02	80.3	TBD	(20 y)	$2.82 \cdot 10^{-5}$
2B-20[3]	0.17	20.1	0.02	79.7	TBD	(20 y)	$5.65 \cdot 10^{-5}$

[1] Values from CRM-630 certificate (2013) [2]. [2] Values from IRMM1000a certificate [4]. [3] Estimated values based on targeted CRM mixing ratios.

The use of the 1A/1B particles from the previous production campaign turned out to be too low in its ^{230}Th amount per particle (mean particle diameter of about 1 micrometer). Test measurements at NIST clearly showed that the Th contents are not measurable in 1 micron-sized particles. Consequently, PNNL has since tailored its particle synthesis procedure to achieve particles up to 5 microns in diameter. Figure 11 shows the ^{230}Th in-growth after ten years for varying ^{234}U contents of different CRMs based on particles ranging from 1-5 microns in size. A Python script was written to predict likely concentrations of ^{230}Th in several different CRMs as a function of time using the radioactive decay Python library to guide the development of new standards for ages in the range of zero to ten years. The script was written to be flexible, pulling data on CRM compositions and likely production dates from a database built from certificate data and offering the option of plotting data as a function of age and composition for the $^{234}U/^{230}Th$ chronometer. Using the separation strategy described above, sets of particles could be prepared from repurified material and then synthesized to a prescribed size distribution.
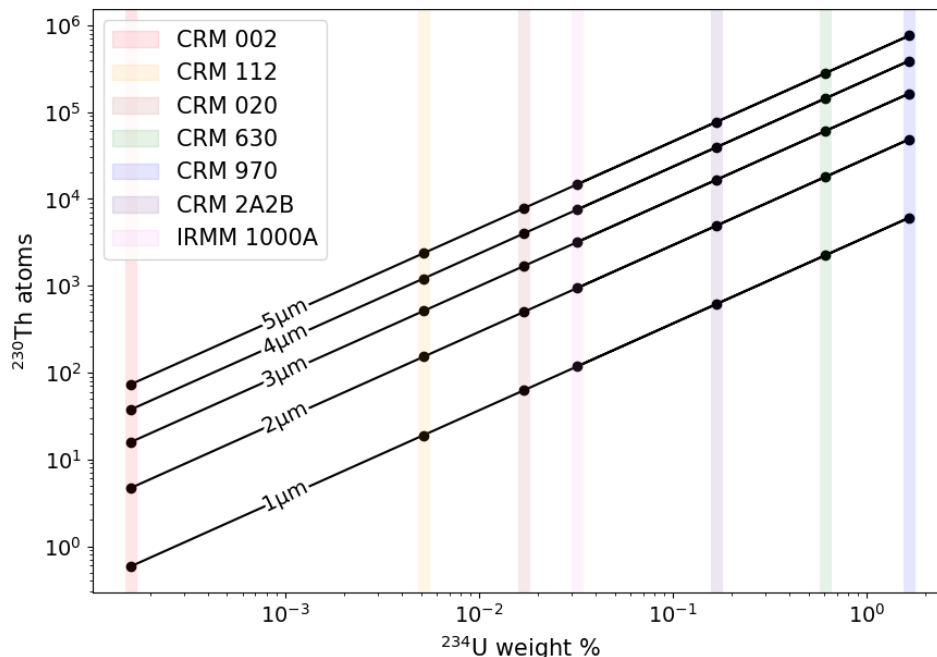
Figure 11. ^{230}Th ingrowth after ten years in particles with sizes between 1-5 micron as a function of the uranium's ^{234}U contents. Assuming complete Th separation from U at time T=0 years.

To this end, PNNL has requested input from the IAEA on the ^{234}U/^{230}Th composition of the final products from CRM-630, IRMM-1000a, as well as the 2A/2B formulations, as described above, and the targeted particle sizes needed for age-dating measurements. While three specific blends of enriched material are highlighted, other formulations and enrichments can be made available using a similar strategy demonstrated for the 1A/1B production cycle. That said, additional time would be needed to prepare any unique uranium formulations.

U/Pu Particle Generation R&D and Development Activities

The project focus for SRNL and LANL in FY21 centered on several tasks in support of maturation U/Pu mixed element reference particulate production technologies and was structured via serial stepwise efforts to minimize technical and operational risk. Most R&D performed supports eventual manufacturing and qualification of IAEA-requested U/Pu particle reference specimens identified as 3A and 3B, these activities included:

- Engineering upgrades to the existing SRNL-developed Monodisperse Particle Production and Collection System (MPPaCS) with inline calcination and substrate deposition masking capabilities. This new version of the production platform was named the THermally Evaporated Spray for Engineered Uniform particulateS (THESEUS).
- New Pu material feedstocks were required for future 3A/3B production. Ergo the sourcing, purification, and characterization of two unique Pu material feedstocks was conducted with a technical memorandum generated for one of the materials entitled "Purification of a Plutonium-240 Source to Generate SRM #Pu-240-98-2021" with doc# SRNL-RP-2021-04359.
- The synthesis of U/Th surrogacy particle test materials via THESEUS and their characterization via LG-SIMS to assess interparticle homogeneity for the production method. Efforts were documented in a technical report entitled "Production of Mixed Element Actinide Reference

Particulates for Nuclear Safeguards Test Materials by an Aerosol Synthesis Method" and Doc# SRNL-TR-2021-00663

Other project activities included the completion of LEU reference particulates reporting and delivery to the IAEA and startup of new inkjet particle production technology, which included:

- The completion of LEU formulation 1A and 1B, their qualification, and delivery to the IAEA. The final qualification report was entitled "Particle Standards Report for the Production of 1A and 1B Material" with doc# SRNL-STI-2021-00070 and was delivered to the IAEA. A complimentary peer review publication was presented at the 2021 INMM & ESARDA Joint Virtual Annual Meeting and entitled "Scale-up And Production Of Uranium-bearing QC Reference Particulates By An Aerosol Synthesis Method" with doc# SRNL-STI-2021-00350. The potential publication document was written without proprietary 1A and 1B isotopic composition information.
- Procurement, setup, and initial testing of particle inkjet printing technology transferred from NIST in FY21. These activities were reported in a technical memorandum entitled "Status Update for NA-24 - Development of New Particle Working Standards for NWAL Particle Laboratory Calibration and Quality Control" with doc# SRNL-TR-2021-00661.

Mixed element U/Th particle production as a surrogate for U/Pu compositions were explored in FY21 completed with a combination particle syntheses and LG-SIMS mixed element measurements which demonstrated interparticle elemental ratio homogeneity. These efforts resulted in refined particle generation methods and feedstock preparation routes for the production of thorium-bearing uranium particulates which may be applied to further development of U/Pu particles. In support of these development activities, SRNL generated a series of 1-micron U/Th particulates across a range of Th compositions, spanning 1 ppm to 10% Th-to-U ratio), and delivered them to LANL for additional characterization using LG-SIMS. Early FY21 development efforts included modifications to the SRNL-developed Monodisperse Particle Production and Collection System (MPPaCS) to include inline heating, enabling the thermal conversion of the produced particulates to a more stable oxide phase. This modified MPPaCS design, referred to as the THermally Evaporated Spray for Engineered Uniform particulateS (THESEUS) production platform, served as the basis for both U/Th and future U/Pu development efforts and is shown in Figure 12.
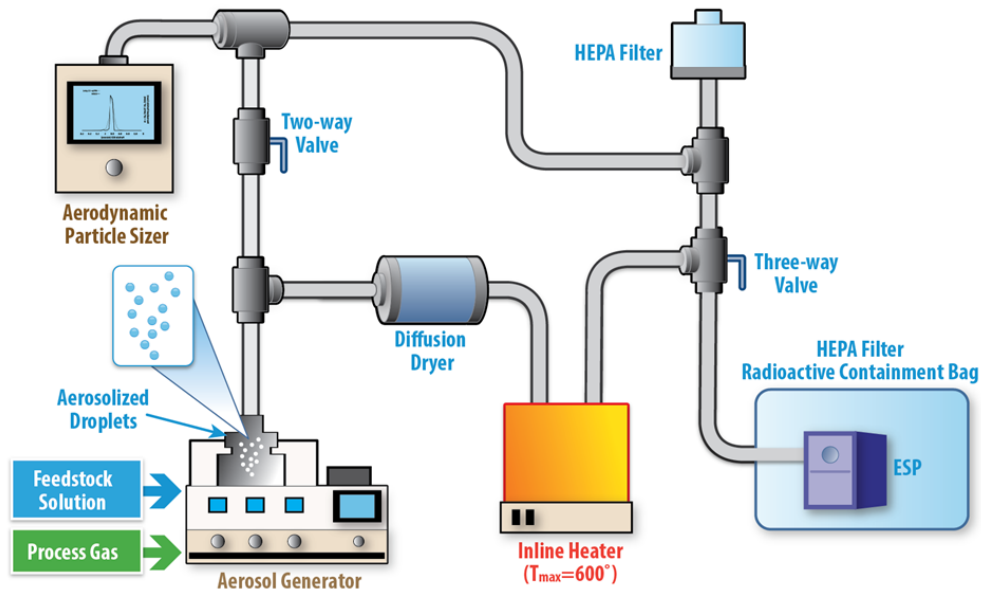
Figure 12 Diagram of the THermally Evaporated Spray for Engineered Uniform particulateS (THESEUS) production platform used in the development of U/Th and U/Pu particulates.

While the switch to THESEUS enabled the generation of uranium oxide particles through the inline heating of the uranium-bearing aerosols, additional refinement was required to maintain the particle qualities obtained for uranyl oxalate particles generated using the MPPaCS. Initially, uranyl nitrate feedstocks were used to improve the shelf-life of the starting solutions, however the emergence of <100 nm "satellite" particles in the generated particle populations resulted in the decision to use uranyl oxalate feedstocks for uranium oxide production, maintaining the monomodal size distributions of the generated particles. Additionally, modifications to the particle generation routines included the modification of feedstock solution concentrations to compensate for the large change in density from uranyl oxalate (3.07 g/cm^3) to U_3O_8 (8.30 g/cm^3). To maintain the target 1-μm equivalent circular diameter (ECD) in uranium oxide particles, and further compensate for the underestimation of particle size during 1A/1B production, the concentration of uranyl oxalate feedstock solution was increased from 8.15 x 10^{-5} vol./vol. to 2.75 x 10^{-4} vol./vol. ratio. This resulted in uniformly monodisperse particles (GSD ≤ 1.10) and particle sizes reproducibly near 1-μm ECD, as shown in Figure 13.
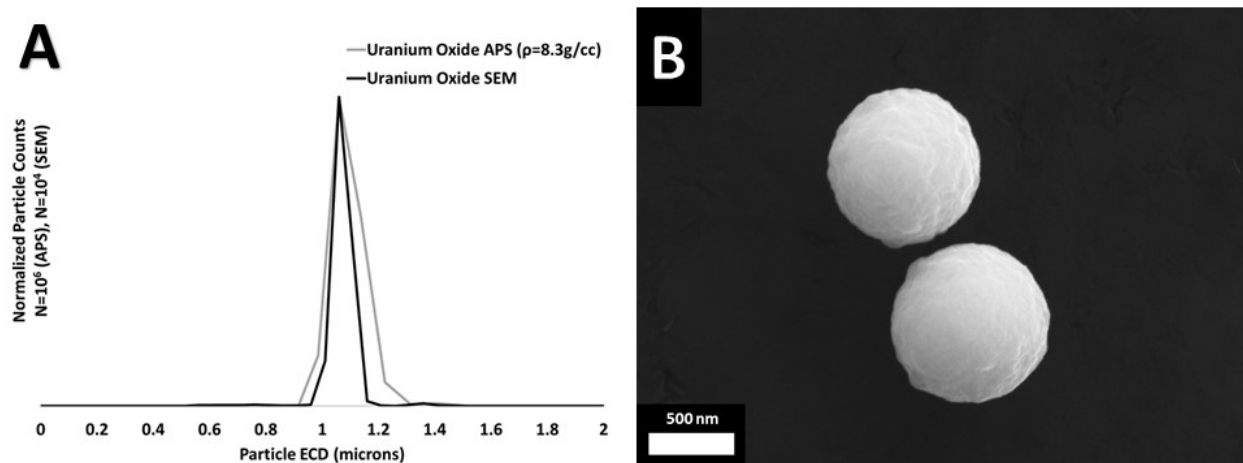
Figure 13 (A) Comparison of APS and APM SEM size distributions for uranium oxide particles generated at 600 °C, (B) exemplar uranium oxide particulates.

The generation of mixed-element U/Th particles in support of U/Pu method development involved the generation of uranium oxide particles with varying amounts of Th incorporation, ranging from 1 ppm to 10% Th-U ratio. Aerodynamic and SEM measurements of particle size displayed a retention of monodispersity and average particle size with increasing Th content (Figure 14).
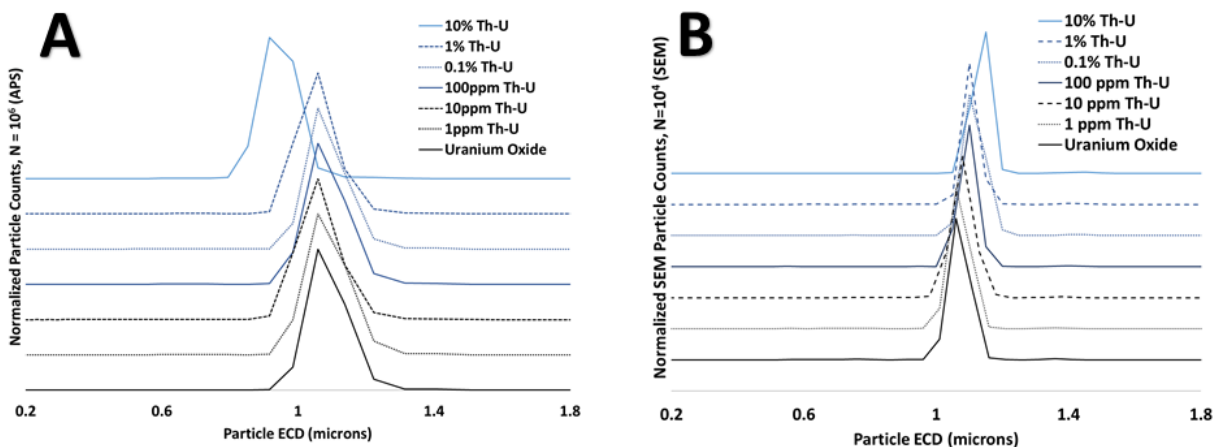

Figure 14 (A) Aerodynamic particle size profiles, and (B) APM SEM size distributions of mixed uranium-thorium particulates of varying Th content.

Notably, particles with 10% Th-U displayed a small change (approx. 0.10 μm) in mean ECD as compared to uranium oxide particles. The deviation in APS and SEM measurements may be explained by a decrease in density of the 10% Th-U particulates, as shown in Figure 15. Despite this small deviation for elevated Th contents, the high degree of monodispersity and agreement in particle size demonstrates the capability of THESUS to generate uniform test particulates of varying Th-U contents (Table 4).
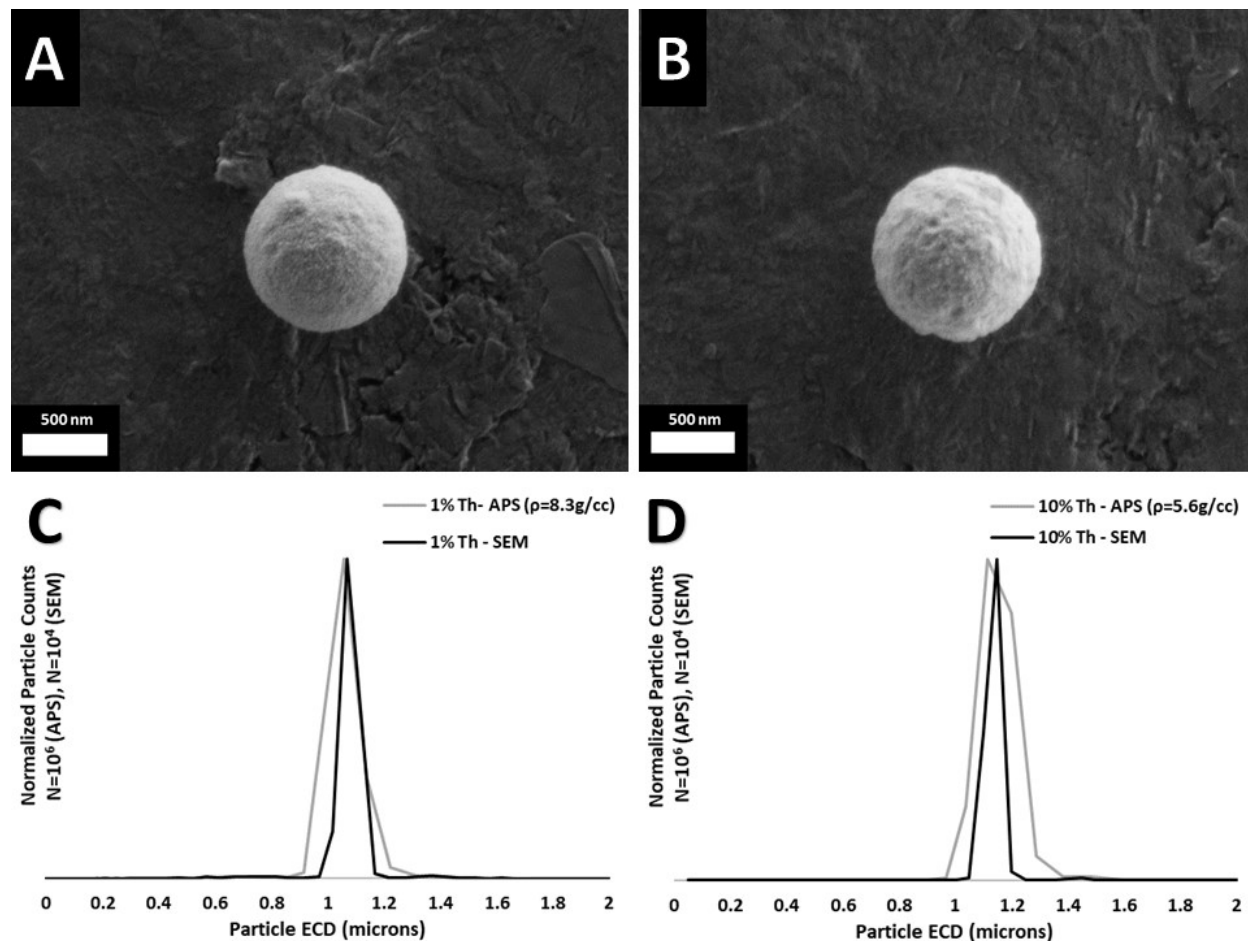
Figure 15 Exemplar particulates of (A) 1% Th-U ratio, (B) 10% Th-U ratio. Comparison of APS and APM SEM size distributions for particles of (C) 1% Th-U ratio, (D) 10% Th-U ratio.

Table 4 Measured aerodynamic and SEM size distribution results of the generated uranium-thorium particulates, including the calculated densities obtained by the reconciliation of APS and APM SEM sizing results.

Sample ID	Composition	APS d_{avg} (µm)	APS GSD (σ_G)	SEM d_{avg} (µm)	ρ_{calc} (g/cm³)
20271	Uranium Oxide	1.05	1.08	1.03	8.3
20280	1 ppm Th / U	1.05	1.08	1.05	8.3
20286	10 ppm Th / U	1.05	1.09	1.1	8.3
20292	100 ppm Th / U	1.05	1.10	1.1	8.3
20298	0.1% Th / U	1.05	1.09	1.1	8.3
20304	1% Th / U	1.05	1.09	1.07	8.3
20316	10% Th / U	1.15	1.10	1.15	5.6

Additional refinement of THESEUS towards U/Pu particle generation includes the development of collection techniques to meet the low particle loadings (500 to 2000 particles within a 10-mm diameter region) specified in the request for 3A/3B materials. Efforts to limit the placement and number of particles deposited on a substrate involved the development of masked planchet collectors, shown in Figure 16A.

The masked collectors minimize the number of stray particles which can be deposited on a substrate, limiting the collection region to the designated 10-mm diameter central region. By using the masked collector and adjusting the collection time, production routines were developed to ensure the number of particles collected on the substrate met the target specifications of 500 to 2000 particles per substrate, as confirmed by automated SEM of the substrate and demonstrated in Figure 16B.
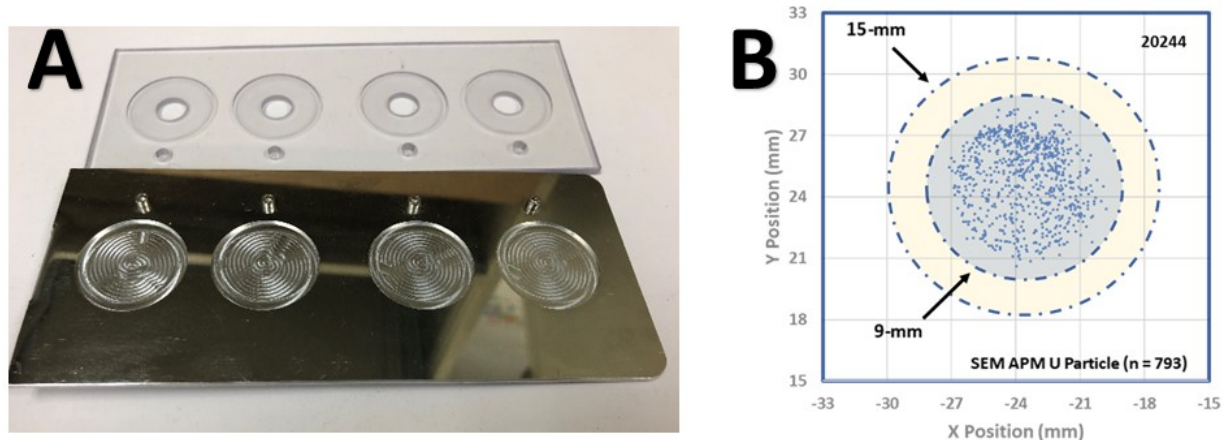

Figure 16 A) Optical image of revised masked planchet collection plate design, and (B) an automated SEM-generated particle map of a masked planchet collected for 5 seconds (N=793 particles).

The compiled results of U/Th particle production and characterization by SRNL and LANL are detailed in a technical report, SRNL-TR-2021-00663. Furthermore, the results of the U/Th particle production efforts are expected to serve as the basis for a journal publication, entitled "Aerosol Synthesis Method for the Production of Mixed Element Reference Particulates for Nuclear Safeguards" which is currently in preparation. In late FY21, LANL characterized a second batch of Th/U particles by LG-SIMS. This batch of materials was analogous to a production-level of quality. Single particle measurements were performed via depth profiling analyses of single particles and automated mapping analyses of samples to evaluate the element and isotope homogeneity of samples. Seven particle standards of varying mixed Th and U compositions were characterized by LG-SIMS at LANL. The samples were made from a depleted U feedstock with approximately 0.17% ^{235}U, and a Th feedstock that is >99.8% ^{232}Th (no ^{230}Th could be detected by LG-SIMS). All particle standards characterized were mounted on silicon wafers. The sample IDs and respective compositions that were characterized are shown in Table 4.

Thorium and uranium isotope ratios for individual particles were obtained with the LANL Cameca IMS-1280 large geometry secondary ion mass spectrometer (LG-SIMS). Ten to eleven particles were identified and selected for each respective Th-U sample. Particle isotope signals were measured using five multicollector electron multipliers (MC EMS), which counted signals from ^{232}Th, ^{235}U, ^{236}U, ^{238}U and ^{238}U^{1}H simultaneously, Each measurement was collected with a primary beam current of 1 nA, a 10 μm raster size, a field aperture width of 6000 μm, an entrance slit width of 122 μm, a contrast aperture width of 400 μm and an energy slit width of 50 μm. All other secondary ion optics and ion detector parameters were optimized to ensure quality analytical results. With these settings the 238U signal was optimized to 1E5 to 2E5 counts per second (cps).

Each single particle analysis consisted of 240 second dwell time that was split into ten 24-second blocks. Prior to an analysis, the particle was pre-sputtered for 10 seconds using a 25 μm-rastered beam and the

same beam current as the analysis. Final isotope ratios for each particle are calculated using the sum of counts for each isotope. Isotope ratio uncertainties of a given single particle analysis are calculated as the two-standard error (2SE) from the analysis blocks.

Depth profiling measurements of single particles also utilized the multicollection system, with the same configuration, instrument parameters, and beam current as the single particle measurements described above. Each profile analysis was 2100 seconds in duration, but count rates were significantly diminished by 1000 seconds, indicting the particle was consumed. As such plots of depth profiles show only the first 1000 seconds of data from profiles.

Per map analysis, a 30 nA primary ion beam was rastered over a 250 x 250 micron area. The area was sputter cleaned using these conditions for 30 seconds prior to an analysis. Map analyses also utilized the multicollection system, with the same configuration as the single particle and profiling analyses. The total count time per map was 240 seconds, and isotope ratios were calculated from the total counts of each isotope for each particle identified. For each sample, several map analyses were collected to generate large particle datasets, and isotope ratios of identified particles were determined using Cameca's Automated Particle Measurement software. To evaluate the homogeneity of particle datasets we employ a model that predicts the scatter in data about a given isotope ratio:

$$\text{Equation 1: } avg.\ N/D \pm \left(avg.\ N/D \times 3.5 \times \sqrt{\frac{1}{N counts} + \frac{1}{D counts}} \right)$$

This model is based on counting statistics, where N and D represent all possible signal combinations from the numerator and denominator of interest that correspond to the average isotope ratio, and the factor 3.5 represents a Gaussian distribution factor for which 99+% of data should fall inside the upper and lower bounds of the model curves shown in the figures of mapped particle isotope data. Specifically, if a significant number of data plot outside of the model bounds, it indicates the particle population is isotopically heterogeneous for the given isotope ratio.

Figure 17 shows the summary of single particle $^{232}Th/^{238}U$ ratios as a function of their ^{238}U total counts. Each plot shows the 2SD of the average of particle data (dashed lines), along with the counting statistics-based model that predicts the expected scatter of the dataset if the sample is isotopically homogeneous (e.g. Equation 1). Except for sample 20316 (nominal Th/U: 0.1; Figure 17a), all sample 2SD values are similar to or better than the models of expected data scatter for a homogeneous source. For sample 20316 the absolute data scatter exceed the model of expected scatter of isotope homogeneity, although the large individual particle data uncertainties put them in agreement with the model (Figure 17a). We attribute the additional scatter in sample 20316 single particle data to (1) a significant change in the $^{232}Th/^{238}U$ ratio as the LG-SIMS primary ion beam profiles through sample 20316 particles (which is discussed further below); combined with (2) slight differences in the times along the profile for which each single particle was analyzed in sample 20316, due to time differences checking for instrument tuning and alignment prior to each analysis. Taking this into consideration, we contend that sample 20316 has a similar extent of particle-to-particle $^{232}Th/^{238}U$ homogeneity as the other samples.

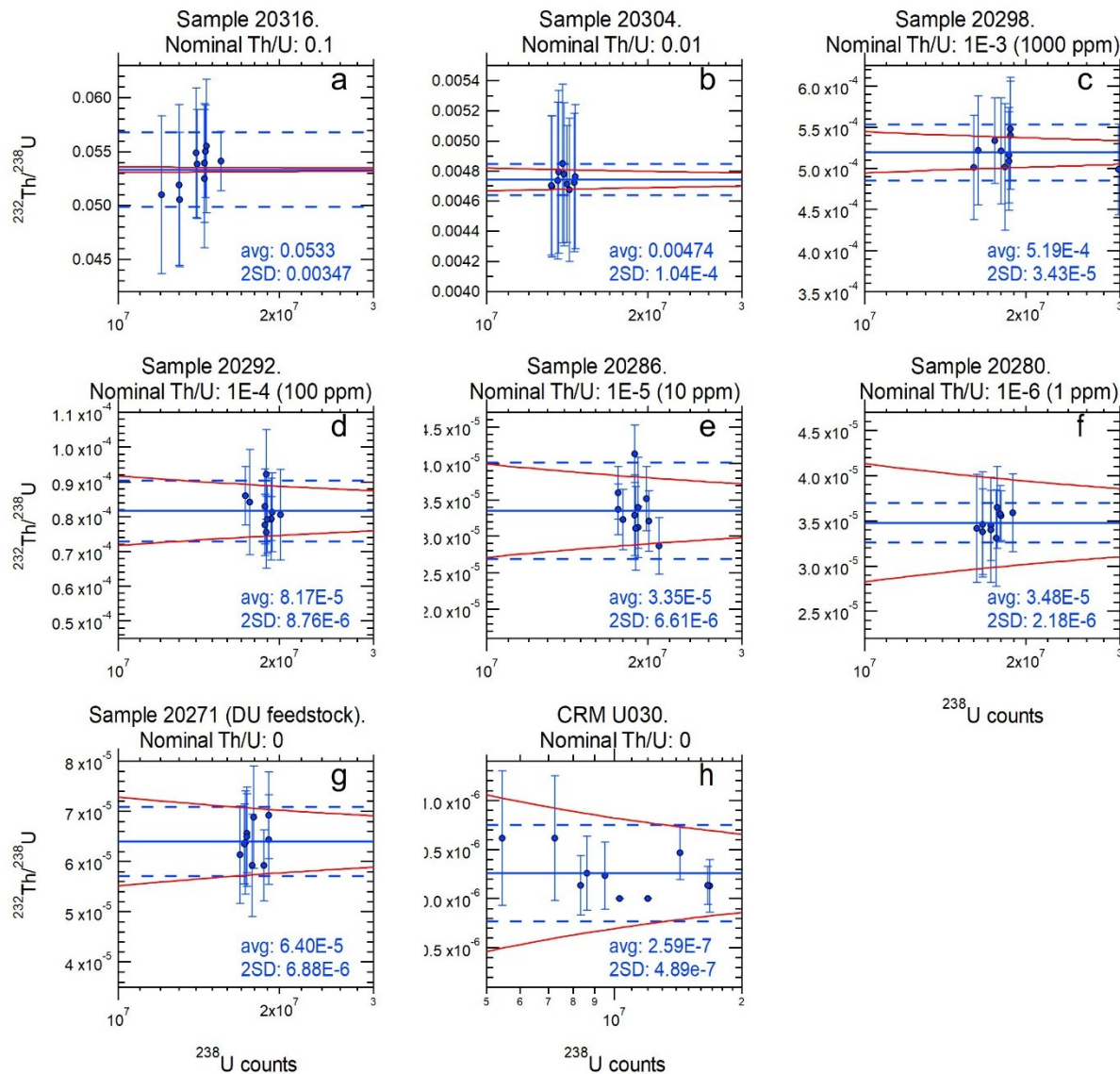*Figure 17: Single particle 232Th/238U vs 238U count data for mixed Th/U samples. Individual error bars are the 2SE of analysis cycles. Dashed lines are the 2SD of the dataset averages. Solid red curves are the counting statistics-based models of expected particle data scatter for a homogeneous material (Equation 1 in the main text).*

Figure 18 shows a comparison of the nominal Th/U ratio versus the average ^{232}Th/^{238}U of single particles measured per sample (as shown in Figure 17). Generally, the samples produce a well-constrained linear regression with an R-squared value approaching unity; the slope of this regression, y = 0.5327x, is effectively the LG-SIMS Th/U relative sensitivity factor (RSF), defined as the ratio of the measured (raw) to the known Th/U ratio of a sample. The observation that all samples effectively produce a linear correlation indicates the LG-SIMS RSF is constant regardless of the Th/U ratio of samples; the regression R-squared value of 0.99985 also suggests that the targeted Th/U ratios of each sample during production are accurate. We note that all sample particles were analyzed using identical instrument parameters, which is critical for making sample-to-sample evaluations in this manner.
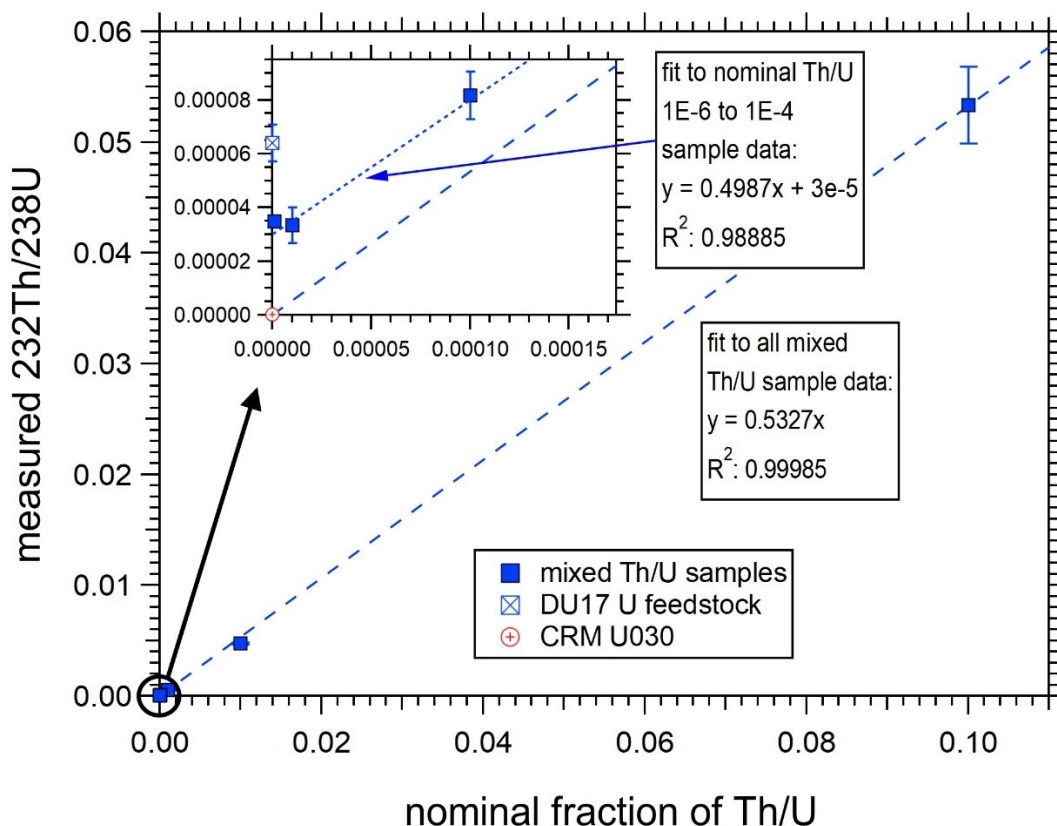
Figure 18: Comparison of the nominal Th/U fraction of samples to the measured average ^{232}Th/^{238}U (given in Figure 17) of mixed Th/U samples. Uncertainties are the 2SD values as reported in Figure 17.

The inset to Figure 18 shows the averages of samples with the lowest Th/U fractions, along with data from the DU feedstock (sample label DU17 in Figure 18) and from certified reference material (CRM) U030. Here, it is observed that the samples with nominal Th/U fractions of 1E-4, 1E-5, and 1E-6 plot slightly above the linear regression for all sample data. In addition, the DU17 feedstock, which should nominally have no Th, has a measured ^{232}Th/^{238}U of ~0.00006, or approximately 60 ppm. This measurement is unlikely to be erroneous, as accompanying measurements of CRM U030 single particles (also nominally having 0 Th) yielded an averaged ^{232}Th/^{238}U value of 2.6($\pm$ 4.9)E-7 (see also: Figure 17h), which is essentially 0. Overall, this indicates that the DU17 feedstock contains a small amount of Th (likely in the low tens of ppm), and that because of this, all samples have a slightly higher abundance of Th than their nominal values. If true, this would influence the samples with the lowest nominal Th/U ratios the most (e.g. samples with nominal values of 100 pp or less), from a relative standpoint; this would explain why these samples plot slightly above the regression line for all sample data as shown in Figure 18.

Figure 19 shows comparison of single particle depth profiles from the samples with the most Th (20316, 20304, and 20298; Table 4). In each plot the ^{232}Th/^{238}U and ^{232}Th signal values are scaled to allow for a visual comparison to the ^{235}U/^{238}U and ^{238}U signal profiles. However, the key observation of these plots is that there is a difference between the ^{232}Th/^{238}U profiling behavior of sample 20316 compared to the other samples with less Th (e.g. a difference in the purple data trend in Figure 19a versus those in Figure 19b and Figure 19c, respectively). Specifically, for sample 20316, there is a sharp increase in the

232Th/238U ratio over the first 120 seconds of the profile, followed by a decrease in the ratio form 120 to 600 seconds, followed by another increase in the ratio from 600 to 1000 seconds of the profile analysis. In contrast for all other samples, there is a relatively constant ^{232}Th/^{238}U ratio over the first 120 seconds, followed by an increase in the ratio from ~120 to 200 seconds, and then the ratio remains more or less constant from 20 to 1000 seconds of the analysis (we note that this behavior is also observed for the samples with lower abundances of Th, but their plots are not shown).

If one considers that single particle and map analyses were collected over the first 240 seconds of these profiles (including sputter cleaning steps of 10 seconds and 30 seconds, respectively, prior to counting), these profiles indicate that ^{232}Th/^{238}U ratios of particles changed during analyses for all samples. However, the relative change is greater for sample 20316 particles versus the other particles. This likely explains why 20316 single particle data (e.g. Figure 17) and map data (discussed below) show more relative scatter than data from the other samples. Specifically, the relatively large change in the profiling behavior over time can lead to more scatter in data if each analysis is not started at the same point along the profile. This can easily happen due to differences in the time it takes to tune and align the instrument prior to an analysis, from particle to particle. This also influences the scatter observed among particle data from the other samples, but the extent of this effect is relatively muted for these samples because their ^{232}Th/^{238}U profiles are more constant over time than that for sample 20316. This is especially apparent for mapping data, as discussed in the following section. We note that additional profiles of particles from samples (including sample 20316) showed identical patterns. This means that, if the variability of ^{232}Th/^{238}U ratios when profiling through a particle reflects a level of heterogeneity *within a particle*, this heterogeneity is identical *among the particles of the sample population*. As such, we coin the term "homogeneously heterogeneous" to describe a population of particles from a given sample. An analogy for this term would be a bag of orange candy pops, where each individual piece is heterogeneous insofar in that it consists of a stick, a wrapper, an orange-flavored candy shell, and a chocolaty core. However, every piece in the bag is constructed identically.
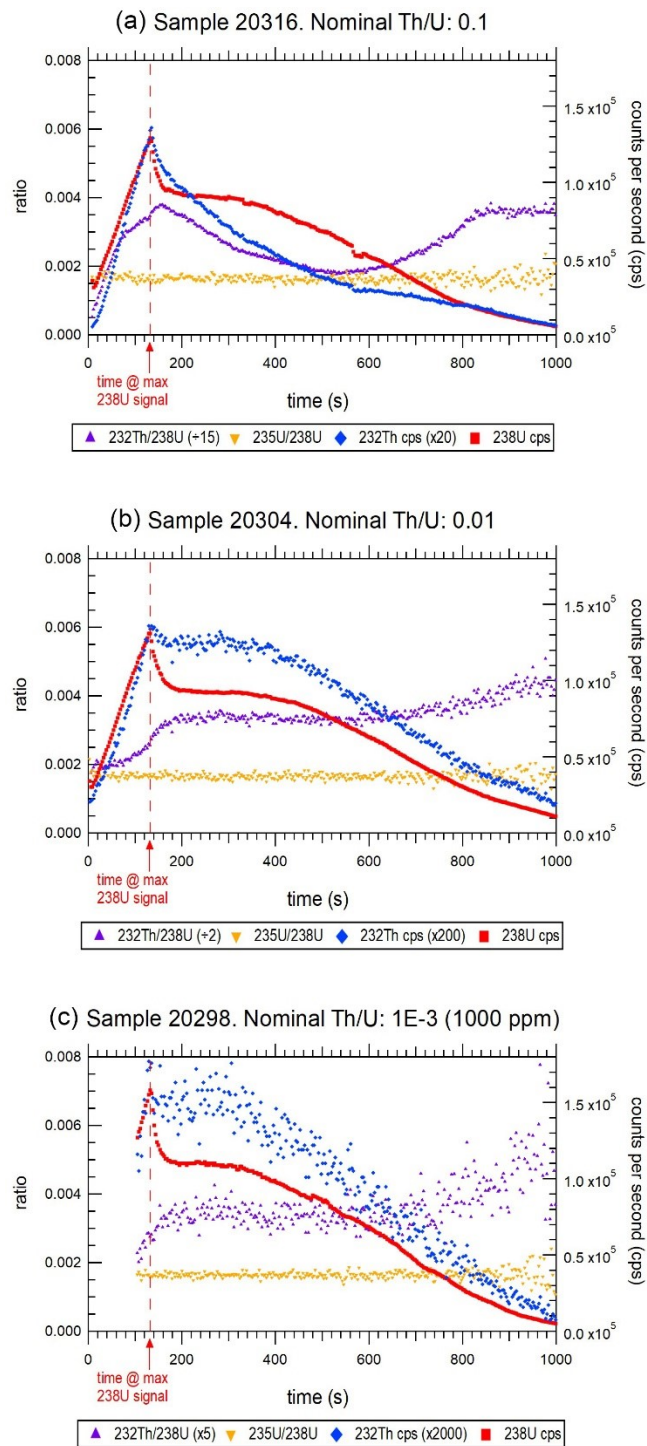
Figure 19: Single particle depth profiles from the three samples with the most Th. The $^{232}Th/^{238}U$ and ^{232}Th signal values are scaled to allow for a visual comparison to the $^{235}U/^{238}U$ and ^{238}U signal profiles.

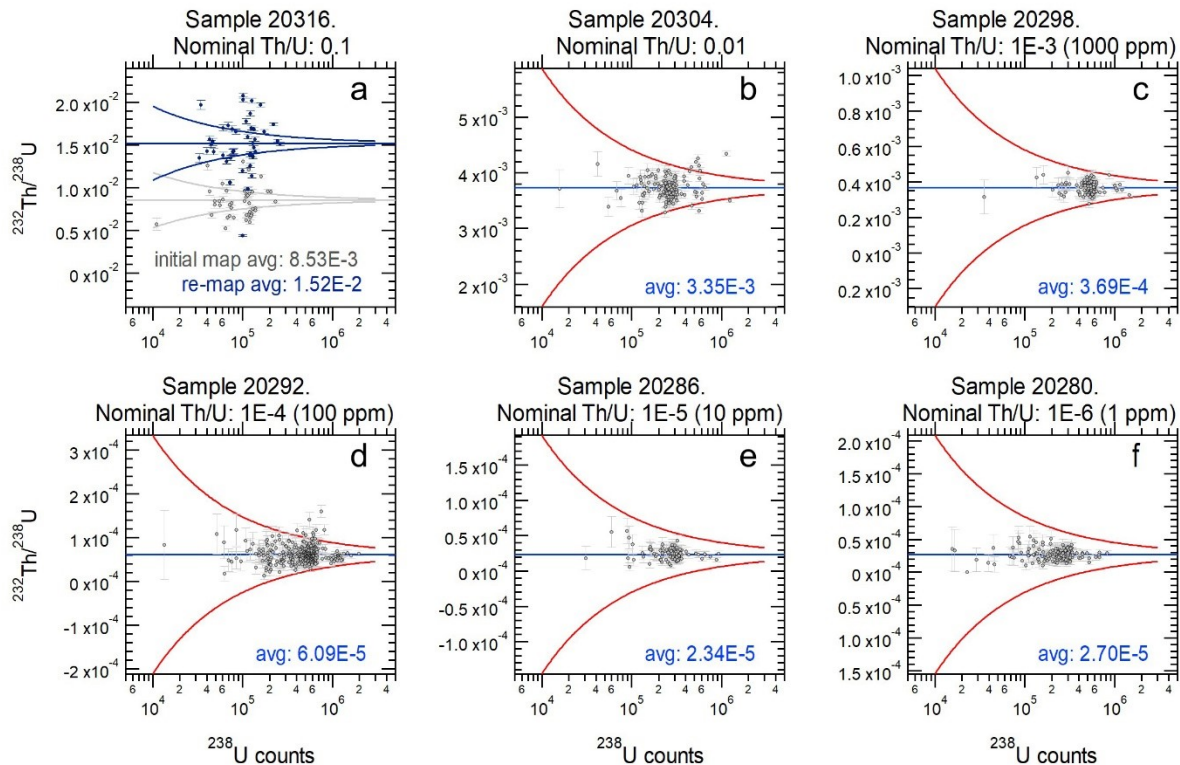*Figure 20: 232Th/238U Mapping data of particle populations from Th/U samples. Red curves are models (e.g. Equation 1) that predict the expected level of data scatter about the average value of the dataset (blue lines) if a sample is isotopically homogeneous.*

Figure 20 shows LG-SIMS isotope mapping data of particle populations of each sample with a nominal finite abundance of Th (the DU17 feedstock and CRM U030 samples were not mapped because they nominally have 0 Th). With the exception of sample 20316, all samples are effectively homogeneous in their ^{232}Th/^{238}U ratios, as few to no particle data plot outside of the model bounds for a given sample. For sample 20316, there is significant scatter in the data outside of the model bounds for the averaged value (Figure 20a). However, this is almost certainly due to the large change in the ^{232}Th/^{238}U ratios of particles over time, as they are being analyzed, as shown in the Figure 19a depth profile. This hypothesis is further supported by a re-mapping of the same area of the 20316 sample, which showed an increase in the average of the dataset (e.g. blue data and model in Figure 20a) when compared to the initially-mapped dataset (e.g. gray data and model in Figure 20a). Finally, we note that the averages of the mapped data are not consistent with the averages of corresponding single particle data for any given sample. However, this is unsurprising because different analytical conditions (e.g. mapping versus single particle analyses) profile through particles at different rates; when one takes this into consideration, along with the fact that the ^{232}Th/^{238}U ratios generally change as they are profiled (e.g. Figure 19), different analysis conditions will lead to different LG-SIMS Th/U relative senility factors. However, regardless of the conditions employed for characterization, as long as the same conditions are applied from sample to sample, meaningful comparisons can be made from sample to sample, at those analytical conditions.

LG-SIMS single particle data and particle map data of mixed Th/U samples reveal that they are homogeneous in ^{232}Th/^{238}U. LG-SIMS depth profiling analyses reveal that ^{232}Th/^{238}U ratios change over time during LG-SIMS analysis. This may indicate that, within a single particle, it may be heterogeneous in

^{232}Th/^{238}U. However, multiple depth profiles of particles of a given sample show identical behavior, confirming that from particle to particle they are homogeneous in their ^{232}Th/^{238}U makeup. As such, we apply the term "homogeneously heterogeneous" as a way to describe a population of particles from a given sample. The analogy here is a bag of orange candy pops, where each individual piece is heterogeneous insofar in that it consists of a stick, a wrapper, an orange-flavored candy shell, and a chocolaty core, but that every piece in the bag is constructed identically.

All the samples are also likely to have their targeted Th/U fractions. This conclusion is based on the fact that the averaged ^{232}Th/^{238}U ratios of single particle datasets per sample produce a well-constrained linear regression when compared to the nominal Th/U fraction of samples. However, the depleted U feedstock used to make the samples likes has a non-zero abundance of Th, at the level of low tens of ppm, which may skew samples with the lowest Th/U fractions above their targeted values. Sample 20316, which has the highest nominal Th/U ratio of all samples investigated (nominal Th/U: 0.1), exhibits more scatter in data than those of the other samples, both for single particle data and for mapping data. This scatter is almost certainly due to a large variability in the Th/U ratio as Sample 20316 particles are being analyzed, based on the particle profiling behavior of this material. However, multiple profiles of sample 20316 exhibit identical behavior, and so we infer that, like all of the other samples, Sample 20316 is homogeneous in ^{232}Th/^{238}U, and has a Th/U ratio the meets its targeted composition.

Initial efforts to qualify SRNL's U/Pu particulate production capability involved the assembly of a THESEUS production platform dedicated to Pu-bearing particulates within a radiological hood in SRNL's CAT2 radiological facility. The assembled THESEUS production platform, shown in Figure 21, in an identical version of the system used in the development of mixed element U/Th particles (Figure 12). This further enabled the transfer of the developed mixed element production methods and system operational experience to the generation of U/Pu particles, minimizing the risk associated with the generation of Pu-bearing particulates.

Figure 21 Photograph of the THESEUS platform for U/Pu particle production installed within the SRNL CAT2 radiological facility.

Initial demonstrations of the dedicated U/Pu THESEUS production platform involved the generation of uranium oxide particles with from a depleted uranyl oxalate feedstock. The qualification of the dedicated THESEUS platform resulted in uranium oxide particles, with similar particulate qualities to those generated

during the earlier method developments for U/Th, including an ECD near 1-µm, monomodal size distribution (GSD < 1.10), and a spherical morphology, as shown in Figure 22.
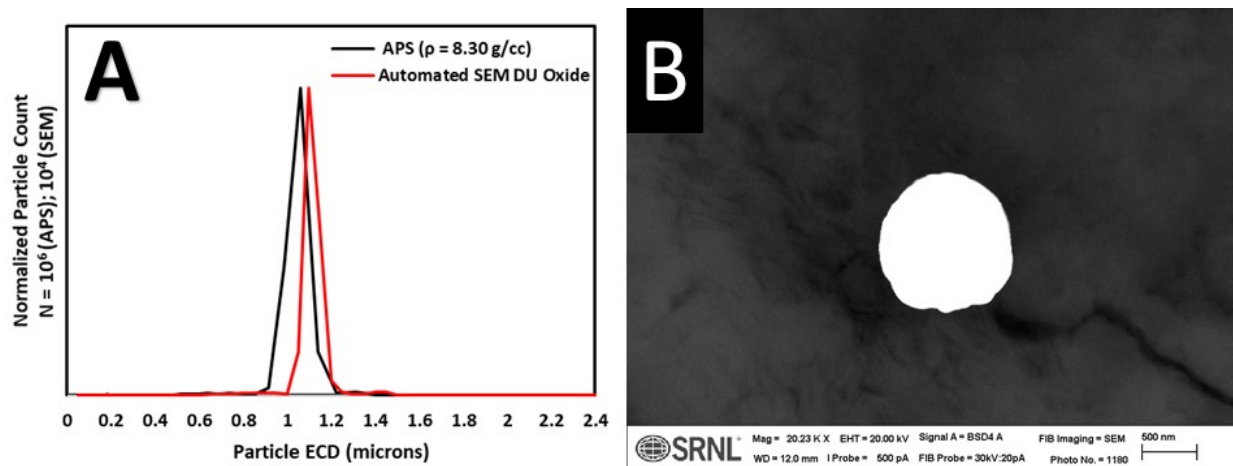

Figure 22 Comparison of aerodynamic and automated SEM particle size distributions for a depleted uranium oxide sample generated on the installed U/Pu system, and (B) high-resolution SEM of a representative DU particle.

Upon the successful demonstration of the newly assembled THESEUS using depleted uranium oxide, initial demonstrations of mixed U/Pu particle production were conducted using the methods developed with the U/Th mixed element system. The demonstration used a depleted uranyl oxalate feedstock with 0.17% [235]U and the recently repurified plutonium feedstock as a plutonium nitrate at U:Pu ratios of 100:1 and 10:1, to serve as surrogates for 3A/3B in testing. Initial demonstrations of U-Pu particle production (Figure 23) indicate the successful generation of mixed U/Pu particulates, with the generated particles displaying size (near 1-µm), monodispersity (GSD < 1.15), and spherical morphology in-line with uranium oxide and the surrogate U/Th particulates used in method development.
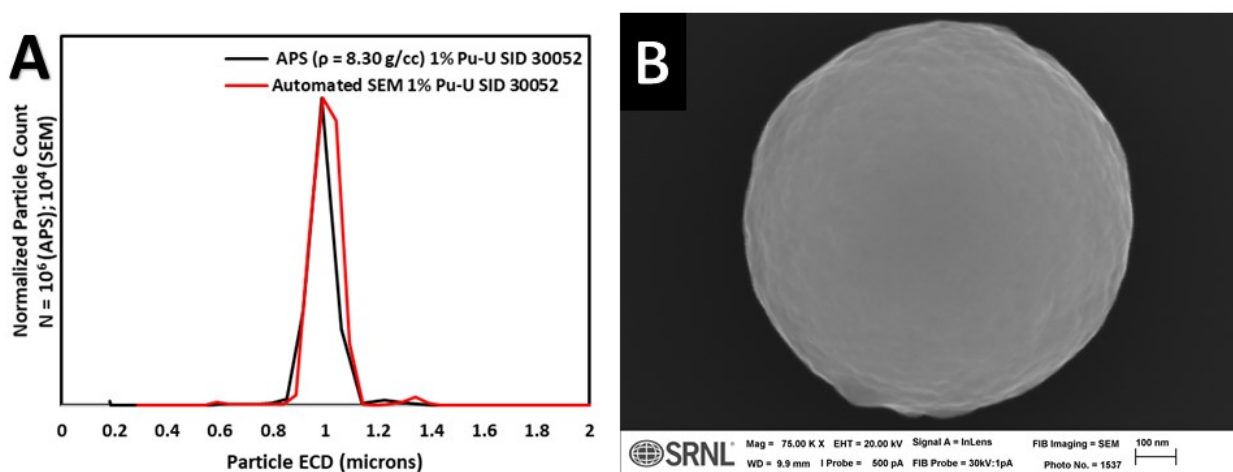

Figure 23 Comparison of APS and APM SEM size distributions for 100:1 U:Pu particles and (B) high-resolution SEM of an exemplar 100:1 U:Pu particle.

Initial assessments of particle concentrations for the generated U/Pu specimens suggest particle loadings within the targets specified for 3A/3B. An example 30 second collection yielded approximately 1500 particles on a 1-inch polished silicon wafer, meeting the 500 to 2000 particle-per-substrate target.

Additional assessments in FY22 will include correlation of alpha spectrometry and automated particle analysis to allow for more rapid screening of the generation of particles to assess particle count and provide a final check of radioactivity for 3A/3B specimens destined for the IAEA's ESL. In Q4 of FY21, two shipments of SRNL-generated U/Pu particulates were sent to LANL to support SIMS characterization.

In addition to the initial demonstration of U/Pu particulate generation, the preparation of Pu feedstocks planned for use in 3A and 3B was initiated in FY21. While FY20 efforts had identified Pu CRMs (C137 and C138) in addition to Pu-240 rich-Pu material at SRNL to generate 3A and 3B feedstocks, shipping latencies were incurred due to the lack of available type B nuclear material shipping containers, required for the transport of the Pu CRMs from the LANL repository to SRNL. To address the shipping latency associated with the Pu CRMs, SRNL identified legacy Pu materials available inhouse to meet project needs for Pu feedstocks. New mixing recipes calculations were conducted using the SRNL-developed Actinide Mixing Optimization Solver (AMOs) for 3A/3B using the SRNL Pu feedstocks or SRMs (Savannah River Materials), and a memo of their composition was generated and shared with SGTech program management and the IAEA, with concurrence obtained in FY21 Q3. The alternative compositions of 3A/3B using the identified SRMs are shown in Table 5. The identification of alternative Pu feedstocks already presents within SRNL enabled the cancellation of the Pu CRM order.

Due to the risk associated with these packaging and transportation uncertainties SRNL devised alternative 3A & 3B feedstock recipes which utilizes only Pu material already present at the Savannah River Site. These alternative recipe formulations are possible because of a newly available Pu material colloquially identified as "Pu_duff" with similar isotopic composition to Pu CRM C137. Essentially, SRNL materials can be used to meet both 3A and 3B objectives in the event of late or unavailability of certified reference materials. Table 5 below describes the isotopics and ratios of interest for the alternative recipes to generate 3A and 3B and Table 6 details of the two Pu isotopic composition of the two salient Pu materials available at SRNL. Table 7 shows the isotopic compositions and ratios for the original formulations of provided to the IAEA which utilize Pu CRMs C137 and C138.

Table 5: Proposed alternative CRM mixtures for 3A/3B and their respective isotopic compositions.

Request ID	CRM Mixture[5]	U-235 (at%)	U-236 Content (at / ppm)[6]	U-235/ U-234 (ratio)	U-238/ Pu-239 (ratio)	Pu-240/ Pu-239 (ratio)	Pu-239 Content (at%)	Pu-241 Content (at%)	Pu-242 Content (at%)
3A	U112a$_{(9549)}$ +U930d$_{(317)}$ +U970$_{(113)}$ +Pu_duff$_{(120)}$ + SRM Pu-240-98-2021 $_{(6)}$	4.758	17	84.11	99.89	0.3005	75.470	0.5592	0.8606
3B	U0002$_{(9886)}$ +U116a$_{(150)}$ +Pu_duff$_{(1246)}$ +	1.411	132	86.554	10.002	0.4505	67.644	0.6937	0.7962

---

[5] The CRM mixture notation consists of a known standard, i.e. U112a, and a subscript containing the relative composition of the standard within the mixture (considering only the atomic composition of U and Pu within the standard, and not weight).

[6] U-236 content is listed in atomic percent, then multiplied by 10^4, to convert to parts U-236 per million U.

	SRM Pu-240-98-2021 (216)							

Table 6: Pu isotopic compositions of the two unique potential recipe feedstock materials available at SRNL.

CRM	Pu-238 Content (atom%)	Pu-239 Content (atom%)	Pu-240 Content (atom%)	Pu-241 Content (atom%)	Pu-242 Content (atom%)
SRM Pu-240-98-2021	0.0440	1.0250	96.8446	1.8386	0.2478
Pu_duff	0.4531	79.1926	18.9678	0.4953	0.8912

Pu240_95 has been decay corrected since its last analysis, and the current isotopics are from values last corrected October 2019. Since this material is already slated for use in 3A & 3B feedstocks purification and subsequent reanalysis was performed in late FY21. The Pu_duff material was last analyzed at SRNL several years ago, was a mixture of Pu materials, and was spiked with Pu-238 and Am-241 for a gas corrosion shelf-life study. Am-241 is >0.50 %wt and would need to be removed and the sample reanalyzed. Once values are reanalyzed, mainly only the Pu-241 content would be expected to change, which does not impact IAEA 3A & 3B requirements. One benefit of utilizing both SRNL Pu feedstocks is the increase of Pu-238 content in 3A & 3B, to values more aligned with expected spent fuel compositions compared to the initial recipe show in Table 3.

Table 7: Original CRM mixtures for 3A/3B and their respective isotopic compositions.

Request ID	CRM Mixture[7]	U-235 Enrichment (atomic%)	U-236 Content (atm/ppm)[8]	U-235/ U-234 (ratio)	U-238/ Pu-239 (ratio)	Pu-240/ Pu-239 (ratio)	Pu-241 Content (atom%)	Pu-242 Content (atom%)
3A	U112a(9549) +U930d(317) +U970(113) +C137(120) + SRM Pu-240-98-2021 (6)	4.758	17	84.062	100.06	0.3018	0.5353	1.1872
3B	U0002(9886) +U116a(150) +C138(1067) + SRM Pu-240-98-2021 (375)	1.411	132	86.554	10.04	0.4543	0.5142	0.0889

---

[7] The CRM mixture notation consists of a known standard, i.e. U112a, and a subscript containing the relative composition of the standard within the mixture (considering only the atomic composition of U and Pu within the standard, and not weight).
[8] U-236 content is listed in atomic percent, then multiplied by 10^4, to convert to parts U-236 per million U.

The purification of the first identified Pu feedstock material (SRM Pu-240-98-2021) was completed in Q3 FY21, and a memo detailing its characterization was generated, SRNL-RP-2021-04359. The purification of the second identified Pu feedstock material was completed in Q3 FY21, with a memo detailing its characterization anticipated for delivery to SGTech program management in Q1 FY22. Further purification and characterization of the U feedstocks for 3A/3B are planned in FY22. Once complete, feedstocks of 3A and 3B will be prepared using the mixtures outlined in Table 5. The generation of the 3A and 3B particulate-laden planchets is planned for late FY22, followed by delivery to LANL for assessment of elemental and isotopic homogeneity using LG-SIMS. Pending LANL's assessment, a final characterization report for 3A and 3B will be generated and delivered to the IAEA along with the planchet specimens.

FY22 Future Plans:

The DOE laboratory team composed of SRNL, PNNL, and LANL will continue method development for, and the production of, fit-for-purpose QC particulates as requested by the IAEA. NIST will continue to provide technical guidance as a collaborative SME role to the effort. In FY22 the planned R&D will be focused on a combination of 1) mixed actinide particle production, 2) formulation of feedstocks with tailored elemental and isotopic composition, 3) advanced analytical methods to characterize development specimens and qualify products, and 4) production and delivery of completed QC particulate for qualified material batches.